RESULTS AND DISCUSSION

Although the translocation of Patient A looked balanced (Fig. 2A) [Hou, 2004], there was actually a relatively large deletion at the 3q13.2 breakpoint region of her derivative chromosome 3. FISH analysis revealed that the 3q proximal end of the deleted segment was confined to 3q11.2 between BAC clones, RP11-12H14, and RP11-481M14, and the distal end to 3q13.31 between RP11-5H2 and RP11-1030E24 (Figs. 2B and 3). Since lacking signals were confirmed for 16 other BACs that are located between the two ends, the deletion extended to approximately 19 Mb in size from 3q11.2 to 3q13.31 (UCSC Genome Browser). As for the other derivative chromosome 12, as two neighbor BAC clones, RP11-412I21, and RP11-55L17, in a contig were identified to cover the 12p11.22 breakpoint, there was no deletion at the breakpoint.

To know whether any other chromosomal aberrations exist in the genome of the five patients examined, whole-genome array CGH was performed. Consequently, the array CGH confirmed in Patient A the presence of the 3q deletion (Fig. 4) without deletions or duplications in any other chromosomes. In Patient D, four regions were suspected to have duplication, but this could not be confirmed by subsequent FISH, because her chromosome preparation was not available. There was no chromosomal aberration in the remaining three patients.

A literature search for deletions for 3q11.2–3q13.31 found eight reported cases [Arai et al., 1982; Jenkins et al., 1985; McMorrow et al., 1986; Okada et al., 1987; Fujita et al., 1992; Genuardi et al., 1994; Ogilvie et al., 1998]. The smallest region of overlap (SRO) for deletion among them is almost confined to 3q12–3q13.31 (Fig. 5). The deletion in one patient (Case 8 in Fig. 5) [Jenkins et al., 1985] was reported to lie between 3q11 and 3q21. However, the exact location of the proximal border in this patient was not clear since either FISH or molecular analysis was not carried out. None but one patient [Arai et al., 1982] had any nose anomaly, and none of the eight patients manifested microphathalmia that is virtually accompanied with arhinia [Graham and Lee, 2006]. The exceptional patient whose deletion involved 3q13–q21 (Case 7, Fig. 5) had alobar holoprosencephaly, arhinia, and cleft lip [Arai et al., 1982]. Although arhinia of this case seems atypical and to be a holoprosencephaly-associated median facial anomaly, the patient might provide possible information for localization of the arhinia locus. If the locus exists at the long arm of chromosome 3, it might be confined to a segment between 3q11.2 and the proximal border of the deletion of Case 8

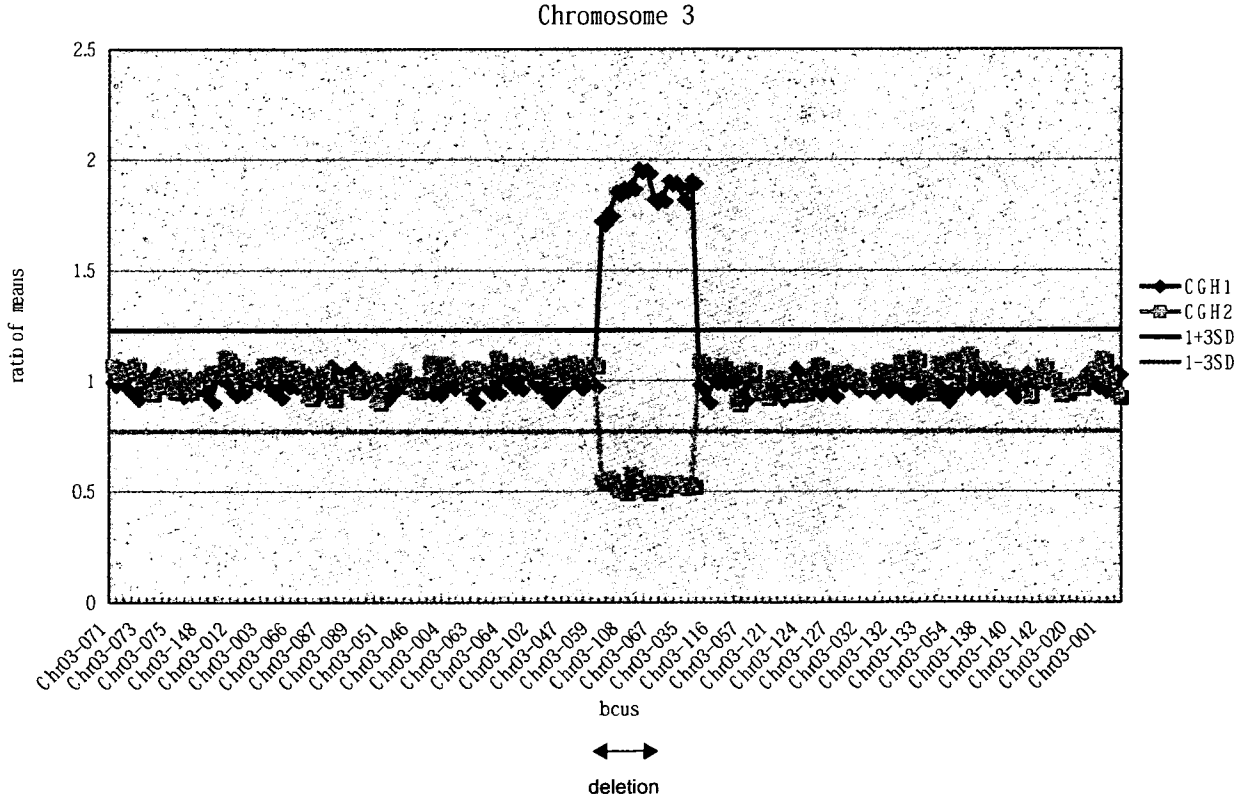

FIG. 4. Array CGH analysis in Patient A, showing a deletion on 3q. The clone at the proximal end within the deletion was RP11-262O19 (3q11.2), and the distal end clone was RP11-342J15 (3q13.31), the results suggesting that the deletion is approximately 18 Mb in size.

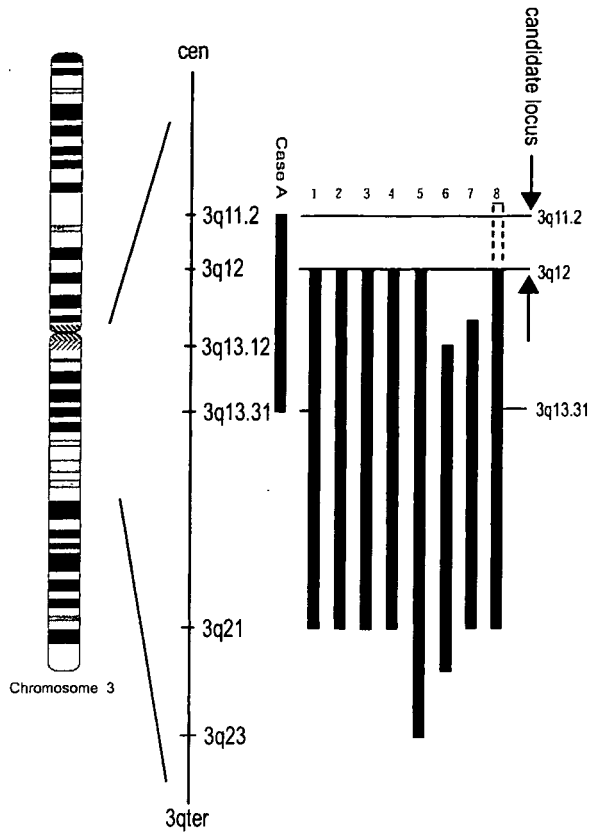

FIG. 5. Extent (bars) of 3q11.2–3q13.31 deletion in Patient A and eight reported cases. **Lanes 1–8** are from McMorrow et al. [1986], Ogilvie et al. [1998], Okada et al. [1987], Fujita et al. [1992], Genuardi et al. [1994], Arai et al. [1982], and Jenkins et al. [1985], respectively.

(Fig. 5). We selected two genes, *COL8A1* and *CPOX*, from 3q11.2 within the deletion of Patient A, and analyzed for their mutations in Patients B–E. According to the Craniofacial and Oral Gene Expression Network (COGENE, http://hg.wustl.edu/COGENE/index.html), *COL8A1* and *CPOX* are expressed in the frontnasal prominence at the 4th week, and between the 4th and 5th weeks, respectively, suggesting they play some roles in the nasal development. However, there was no pathognomonic mutation of *COL8A1* or *CPOX* in the four arhinia patients with normal karyotypes.

As for the other breakpoint of Patient A, we have confirmed that any known genes were not disrupted at 12p11.22. Two genes, *ARG99* and *IPO8*, located near the breakpoint, seem to have no functions related to the human nasal development. However, it cannot totally be ruled out that there may be unknown RNA transcript(s) on the breakpoint or the breakage may affect a long-distance position effect [Velagaleti et al., 2005].

The nasal placode, the anlage of the nose, begins to develop from the 12th to the 13th Carnegie stage, at the end of the fourth embryonic week. The stage between the end of the 4th week to the 7th week is the most active, important period in the human nose development [O'Rahilly, 1967; Kim et al., 2004]. A failure of the developmental process may result in arhinia, for example, failure of growth or overgrowth of the medial and lateral nasal process sequentially leads to premature fusion of the medial nasal processes [Albernaz et al., 1996].

In conclusion, analysis of five patients with arhinia revealed, although a 19 Mb large deletion involving 3q11–q13 was identified in one patient, no chromosome aberrations or gene mutations were found in the other four patients. Nevertheless, our findings may become a clue to isolate the putative arhinia gene. Further molecular studies in new patients, as well as that on other genes within the deleted region in Patient A, are needed to unravel the underlying cause of arhinia. This is the first report of molecular-genetic study on congenital arhinia.

ACKNOWLEDGMENTS

Participation of all patients in this study is highly appreciated. We also thank Ms Y. Noguchi, K. Miyazaki and A. Goto for their technical assistance. This study was supported by Grants-in-Aid for Scientific Research (Category S, No. 13854024 and Priority Areas—Applied Genomics, No. 17019055 for N. N.; and No. 17590288 for K. Y.) from the Ministry of Education, Culture, Sports, Science and Technology (MEXT) of Japan, and by SORST from the Japan Science and Technology Agency (JST) for N. N.

REFERENCES

Albernaz VS, Castillo M, Mukherji K, Ihmeidan IH. 1996. Congenital arhinia. Am J Neuroradiol 17:1312–1314.

Arai K, Matukiyo H, Takazawa H. 1982. A case report of partial deletion of the long arm of the No.3 chromosome. Med Genet Res 4:1–4.

Choi S, Shiozu H, Sato K, Nishida H. 1998. A case report of congenital arhinia. Acta Neonatol Jpn 34:83–86.

Cohen D, Goitein K. 1986. Arhinia. Rhinology 24:287–292.

Cusick W, Sullivan CA, Rojas B, Poole AE, Poole DA. 2000. Prenatal diagnosis of total arhinia. Ultrasound Obstet Gynecol 15:259–261.

Fujita H, Meng J, Kawamura M, Tozuka N, Ishii F, Tanaka N. 1992. Boy with a chromosome del(3)(q12q23) and blepharophimosis syndrome. Am J Med Genet 44:434–436.

Galetti R, Dallari S, Bruzzi M, Vincenzi A, Galetti G. 1994. Consideration on respiratory physiopathology in a case of total arhinia. Acta Otorhinol Ital 14:63–69.

Genuardi M, Calvieri F, Tozzi C, Coslovi R, Neri G. 1994. A new case of interstitial deletion of chromosome 3q,del(3q)(q13.12q21.3), with agenesis of the corpus callosum. Clin Dysmorphol 3:292–296.

Graham JM, Lee J. 2006. Bosma arhinia microphthalmia syndrome. Am J Med Genet Part A 140A:189–193.

Hou JW. 2004. Congenital arhinia with de novo reciprocal translocation, t(3;12)(q13.2;p11.2). Am J Med Genet Part A 130A:200–203.

Jenkins MB, Stang HJ, Davis E, Boyd L. 1985. Deletion of the proximal long arm of chromosome 3 in an infant with features of Turner syndrome. Ann Génét (Paris) 28:42–44.

Jules AF, Cynthia MG, Terry T, Samue S, Brian S, Larry H. 2004. Vertical facial distraction in the treatment of arhinia. Plast Reconstr Surg 113:2061–2066.

Kaminker CP, Dain L, Lamas MA, Sanchez JM. 1985. Mosaic trisomy 9 syndrome with unusual phenotype. Am J Med Genet 22:237–241.

Kim CH, Park HW, Kim K, Yoon JH. 2004. Early development of the nose in human embryos: A stereomicroscopic and histologic analysis. Laryngoscope 114:1791–1800.

Mathur NN, Dubey NK, Kumar S, Bothra R, Chadha A. 2005. Arhinia. Int J Pediatr Otorhinolaryngol 69:97–99.

McGlone L. 2003. Congenital arhinia. J Paediatr Child health 39:474–476.

McMorrow LE, Reid CS, Coleman J, Medeiros A, D'Andrea M, Santucci T, McCormack MK. 1986. A new interstitial deletion of the long arm of chromosome 3. Am J Hum Genet 39: A124.

Miyake N, Shimokawa O, Harada N, Sosonkina N, Okubo A, Kawara H, Okamoto N, Ohashi H, Kurosawa K, Naritomi K, Kaname T, Nagai T, Shotelersuk V, Hou JW, Fukushima Y, Kondoh T, Matsumoto T, Shinoki T, Kato M, Tonoki H, Nomura M, Yoshiura K, Kishino T, Ohta T, Niikawa N, Matsumoto N. 2006. No detectable genomic aberrations by BAC array CGH in Kabuki make-up syndrome patients. Am J Med Genet Part A 140A:291–293.

Mizuguchi T, Collod-Beroud G, Akiyama T, Harada N, Morisaki T, Abifadel M, Allard D, Varret M, Claustres M, Ihara M, Kinoshita A, Yoshiura K, Junien C, Kajii T, Jondeau G, Niikawa N, Boileau C, Matsumoto N. 2004. Heterozygous *TGFBR2* mutations in Marfan syndrome. Nat Genet 36:855–860.

Muhlbauer W, Schmidt A, Fairley J. 1993. Simultaneous construction of an internal and external nose in an infant with arhinia. Plast Reconstr Surg 91:720–725.

O'Rahilly R. 1967. The early development of the nasal pit in staged human embryos. Anat Rec 157:380.

Ogilvie CM, Rooney SC, Hodgson SV, Berry AC. 1998. Deletion of chromosome 3q proximal region gives rise to a variable phenotype. Clin Genet 53:220–222.

Okada N, Hasegawa T, Osawa M, Fukuyama Y. 1987. A case of de novo interstitial deletion 3q. J Med Genet 24:305–308.

Olsen OE, Gjelland K, Reigstad H, Rosendahl K. 2001. Congenital absence of the nose: A case report and literature review. Pediatr Radiol 31:225–232.

Onizuka T, Ohkubo F, Hosaka Y, Ichinose M, Keiko Okazaki K. 1995. Arhinia: A case report. Worldplast 1:65–71.

Ruprecht KW, Majewski F. 1978. Familial arhinia combined with Peter's anomaly and maxillar deformities, a new malformation syndrome? Klin Mbl Augenheilk 172:708–715.

Sakai Y, Ohara Y, Inoue Y. 1989. Congenital complete absence of the nose. J Jpn Plast Reconstr Surg 9:265–273.

Sambrook J, Russell DW. 2001. Molecular cloning: A laboratory manual. Cold Spring Harbor, New York: Cold Spring Harbor Laboratory Press.

Shimokawa O, Miyake N, Yoshimura T, Sosonkina N, Harada N, Mizuguchi T, Kondoh S, Kishino T, Ohta T, Remco V, Takashima T, Kinoshita A, Yoshiura K, Niikawa N, Matsumoto N. 2005. Molecular characterization of del(8)(p23.1p23.1) in a case of congenital diaphragmatic hernia. Am J Med Genet Part A 136A:49–51.

Shino M, Chikamatsu K, Yasuoka Y, Nagai K, Furuya N. 2005. Congenital arhinia: A case report and functional evaluation. Laryngoscope 115:1118–1123.

Thiele H, Musil A, Nagel F, Majewski F. 1996. Familial arhinia, choanal atresia, and microphthalmia. Am J Med Genet 63:310–313.

Velagaleti GVN, Bien-Willner GA, Northup JK, Lockhart LH, Hawkins JC, Jalal SM, Withers M, Lupski JR, Stankiewicz P. 2005. Position Effects due to chromosome breakpoints that map ~900 kb upstream and ~1.3 Mb downstream od SOX9 in two patients with Campomelic dysplasia. Am J Hum Genet 76:652–662.

MOLECULAR AND CELLULAR BIOLOGY, Jan. 2007, p. 732–742 Vol. 27, No. 2
0270-7306/07/$08.00+0 doi:10.1128/MCB.01329-06

Role of DNA Methylation and Histone H3 Lysine 27 Methylation in Tissue-Specific Imprinting of Mouse *Grb10*▽

Yoko Yamasaki-Ishizaki,[1,2,8] Tomohiko Kayashima,[1] Christophe K. Mapendano,[1] Hidenobu Soejima,[3] Tohru Ohta,[4,8] Hideaki Masuzaki,[2] Akira Kinoshita,[1,8] Takeshi Urano,[5] Ko-ichiro Yoshiura,[1,8] Naomichi Matsumoto,[6] Tadayuki Ishimaru,[2] Tsunehiro Mukai,[3] Norio Niikawa,[1,8] and Tatsuya Kishino[7,8]*

Departments of Human Genetics[1] and Obstetrics and Gynecology,[2] Graduate School of Biomedical Sciences, Nagasaki University, Nagasaki, Japan; Department of Biomolecular Sciences, Saga University, Saga, Japan[3]; The Research Institute of Personalized Health Sciences, Health Sciences University of Hokkaido, Hokkaido, Japan[4]; Department of Biochemistry II, Graduate School of Medicine, Nagoya University, Nagoya, Japan[5]; Department of Human Genetics, Graduate School of Medicine, Yokohama City University, Yokohama, Japan[6]; Division of Functional Genomics, Center for Frontier Life Sciences, Nagasaki University, Nagasaki, Japan[7]; and CREST, Japan Science and Technology Agency, Kawaguchi, Japan[8]

Received 19 July 2006/Accepted 24 October 2006

Mouse *Grb10* is a tissue-specific imprinted gene with promoter-specific expression. In most tissues, *Grb10* is expressed exclusively from the major-type promoter of the maternal allele, whereas in the brain, it is expressed predominantly from the brain type promoter of the paternal allele. Such reciprocally imprinted expression in the brain and other tissues is thought to be regulated by DNA methylation and the Polycomb group (PcG) protein Eed. To investigate how DNA methylation and chromatin remodeling by PcG proteins coordinate tissue-specific imprinting of *Grb10*, we analyzed epigenetic modifications associated with *Grb10* expression in cultured brain cells. Reverse transcriptase PCR analysis revealed that the imprinted paternal expression of *Grb10* in the brain implied neuron-specific and developmental stage-specific expression from the paternal brain type promoter, whereas in glial cells and fibroblasts, *Grb10* was reciprocally expressed from the maternal major-type promoter. The cell-specific imprinted expression was not directly related to allele-specific DNA methylation in the promoters because the major-type promoter remained biallelically hypomethylated regardless of its activity, whereas gametic DNA methylation in the brain type promoter was maintained during differentiation. Histone modification analysis showed that allelic methylation of histone H3 lysine 4 and H3 lysine 9 were associated with gametic DNA methylation in the brain type promoter, whereas that of H3 lysine 27 regulated by the Eed PcG complex was detected in the paternal major-type promoter, corresponding to its allele-specific silencing. Here, we propose a molecular model that gametic DNA methylation and chromatin remodeling by PcG proteins during cell differentiation cause tissue-specific imprinting in embryonic tissues.

Genomic imprinting in mammals describes the situation where there is nonequivalence in expression between the maternal and paternal alleles at certain gene loci, depending on the parental origin. Genomic imprinting plays essential roles in development, growth, and behavior (6, 30, 31). Such parental origin-specific gene regulation is caused by epigenetic modifications that occur during gametogenesis without any nucleic acid changes. One of the well-known epigenetic modifications is DNA methylation. In the imprinted loci, differentially methylated regions between the maternal and paternal alleles are often found and associated with parental allele-specific expression (7). Another well-known epigenetic modification is histone modification, which represents the determinant of epigenetic features associated with imprinted genes. It has been reported that parental origin-specific gene expression on some imprinted genes is determined by DNA methylation and/or histone modifications (12, 13, 16, 23, 29, 40). Polycomb group (PcG) proteins also play an important role in various epigenetic phenomena (3), such as maintaining the silent state of the homeotic genes, maintaining X-chromosome inactivation (36), and silencing imprinted genes in mammals (24, 33). PcG protein complexes are thought to maintain long-term gene silencing during development through alterations of local chromatin structure (3, 27).

Mouse *Grb10* encoding the growth factor receptor-bound protein 10 (Grb10) is an imprinted gene with tissue-specific and promoter-specific expression. In most tissues, the major-type transcript of *Grb10* is expressed exclusively from the major-type promoter of the maternal allele, whereas in the brain, the brain type transcript is expressed predominantly from the brain type promoter of the paternal allele (1, 17). DNA methylation analysis has revealed that the CpG island (CGI) in the brain type promoter (CGI2) was gametically methylated in the oocyte as a primary imprint and remained methylated exclusively on the maternal allele in somatic tissues, while the CpG island in the major-type promoter (CGI1) was biallelically hypomethylated in somatic tissues (see Fig. 1 and 4) (17). Hikichi et al. proposed the model for tissue-specific imprinting of *Grb10* that the major-type transcript is regulated by DNA methylation-sensitive insulator (CTCF) binding in CGI2 and

* Corresponding author. Mailing address: Division of Functional Genomics, Center for Frontier Life Sciences, Nagasaki University, Sakamoto 1-12-4, Nagasaki 852-8523, Japan. Phone: 81-95-849-7120. Fax: 81-95-849-7178. E-mail: kishino@net.nagasaki-u.ac.jp.
▽ Published ahead of print on 13 November 2006.

the brain type transcript is regulated by putative brain-specific activators (17). They suggested that allelic DNA methylation in CGI2 can orchestrate reciprocal imprinting of the two promoters of the *Grb10* gene. This model was partially supported by the imprinting analysis of knockout mice of the *Dnmt3L* gene, encoding a factor for acquisition of maternal methylation imprint in germ cells (14, 18). In the embryos (*Dnmt3L*$^{m-/-}$), produced from *Dnmt3L*$^{-/-}$ females, maternal chromosome-specific DNA methylation in CGI2 was lost and null expression of the major-type transcript was detected (2). Recently, the PcG protein Eed (embryonic ectoderm development) was identified as a member of a new class of *trans*-acting factors, which regulate the expression of some paternally repressed imprinted genes, *Cdkn1c*, *Ascl2*, *Meg3*, and *Grb10* (24). In *Eed*$^{-/-}$ embryos, the major-type transcript of *Grb10* was biallelically expressed from the major-type promoter without major alteration of DNA methylation in gametically methylated CGI2, albeit various hypomethylated patterns were observed on the paternal allele (24). The expression analysis of these knockout mice suggests that DNA methylation and chromatin remodeling by PcG proteins represent the epigenetic factors that are necessary for establishing and/or maintaining the imprinted expression of *Grb10*. It remains unknown how they coordinate the tissue-specific and promoter-specific imprinting of *Grb10*.

Recently, mouse genes with brain-specific imprinting patterns were reported. They are *Ube3a* and *Murr1*, with neuron-specific and brain developmental stage-specific expressions, respectively. *Ube3a* is biallelically expressed in most tissues but expressed exclusively from the maternal allele only in neurons, leading to apparent partial imprinting with predominant maternal *Ube3a* expression in the whole brain (38). *Murr1* is imprinted in the adult brain, especially in mature neurons, but not in embryonic and neonatal brains (37). These lines of evidence suggest that brain-specific imprinting may be regulated in part by epigenetic modifications, depending on specification and maturation of cell lineages in the developing brain (9, 19).

Since *Grb10* is a tissue-specific imprinted gene, we hypothesized that tissue-specific reciprocal imprinting of *Grb10* also depends on cell-specific epigenetic modifications acquired during cell differentiation. To examine our hypothesis, we performed an epigenetic analysis of brain cells with the aid of primary cortical cell cultures, in which neurons or glial cells were cultured separately from products of reciprocal crosses between the C57BL/6 and PWK strains (divergent strains of *Mus musculus*). In each cultured brain cell, *Grb10* expression and epigenetic factors such as DNA methylation and histone modifications were analyzed to investigate how DNA methylation and chromatin remodeling by PcG proteins establish and maintain the tissue-specific and promoter-specific imprinting of *Grb10*.

MATERIALS AND METHODS

Mice. All procedures were performed with approval from the Nagasaki University Institutional Animal Care and Use Committee. F_1 hybrid mice were obtained by mating C57BL/6 females with PWK males [(C57BL/6 × PWK)F_1] and vice versa [(PWK × C57BL/6)F_1]. Telencephalon/cerebral cortices and embryonic fibroblasts were prepared from embryonic day 10 (E10) to E15. Tissues were used for RNA and DNA extraction or primary cultures. Brain tissue for reverse transcriptase (RT) PCR was dissected at E10, E16, postnatal day 1, postnatal day 5, 2 weeks, 4 weeks, 6 weeks, and 14 months.

Primary culture. Methods of primary cultures of cortical neurons, glial cells, and embryonic fibroblasts have been described elsewhere (38). In brief, E15 cerebral cortices without meninges were trypsinized to dissociate brain cells. For neuronal culture, dissociated cells were cultured in neurobasal medium (Gibco BRL, Carlsbad, CA) with B27 supplement (Gibco BRL). Cultures were maintained in 5% CO_2 at 37°C for 5 days. For the long culture, half of the culture medium was changed every 3 to 4 days. For glial cell culture, dissociated brain cells were cultured overnight in Dulbecco's modified Eagle's medium (Sigma, St. Louis, MO) supplemented with 10% fetal calf serum, and then the medium was changed to Neurobasal medium (Gibco BRL) with G5 supplement (GIBCO BRL). After 5 to 7 days in the primary culture, cultured glial components were subcultured. Cultures were maintained in 5% CO_2 at 37°C for a total of 14 days. For embryonic fibroblast culture, embryonic fibroblasts derived from E15 embryonic skin were cultured in Dulbecco's modified Eagle's medium supplemented with 10% fetal calf serum.

cDNA synthesis. Total RNA was isolated from cultured cells and tissues with RNeasy (QIAGEN, Hilden, Germany) according to the manufacturer's protocol. The RNA was treated with amplification grade DNase I (Invitrogen, Carlsbad, CA) to degrade any genomic DNA present in the sample. The cDNA was generated from total RNA by SuperScript II reverse transcriptase (Invitrogen) primed with oligo(dT)$_{12-18}$ primers. The first-strand cDNA was synthesized at 42°C for 50 min. Then, mRNA-cDNA chains were denatured and the reverse transcriptase activity was arrested by heating at 70°C for 15 min. An identical reaction was carried out without reverse transcriptase as a negative control.

RT-PCR for expression analysis. The cDNA obtained was used to perform RT-PCR for expression analysis. The expression of each *Grb10* transcript was analyzed using primers 1aF and 1R for the major-type transcript and using primers 1bF and 1R for the brain type transcript. Other transcripts, including exon 1c, were amplified by primer sets 1cF/e2R and 1aF/1cR. PCR amplification with primers 1aF and 1R was performed for 32 to 35 cycles of 15 s at 96°C, 20 s at 60°C, and 60 s at 72°C, with primers 1bF and 1R for 32 to 38 cycles of 15 s at 96°C, 20 s at 60°C, and 60 s at 72°C, and with primer sets 1cF/e2R and 1aF/1cR for 35 cycles of 15 s at 96°C, 20 s at 60°C, and 60 s at 72°C. The primers for *Map2*, *Gfap*, and *Gapdh* used for evaluation of the cultured cells have been described elsewhere (38). For a semiquantitative RT-PCR, optimal template cDNA concentrations were determined according to *Gapdh* amplification. PCR products were amplified for 25 to 30 cycles of 15 s at 96°C, 20 s at 55°C, and 30 s at 72°C.

Quantitative analysis of gene expression by real-time PCR. cDNA was applied to real-time PCR for quantitative analysis of each transcript using SYBR green and an ABI Prism 7900 (PE Applied Biosystems, Foster City, CA). PCR was performed on samples at least in triplicate according to the manufacturer's protocol to control for PCR variation. To standardize each experiment, the results were represented as a percentage of expression, calculated by dividing the average value of the expression of the target gene by that of an internal control gene, *Gapdh* (38). The primers used for real-time PCR were primers 1aF and1R for the major-type transcript and primers Q-1bF and Q-1bR for the brain type transcript. Each experiment was repeated with independent RNAs two to three times.

Sequencing for allelic differences. A sequence chromatogram was used to detect allelic differences of PCR products. Parental expression of major/brain type transcripts in the brain and kidney was analyzed by RT-PCR using primer sets 1aF/coR and 1bF/coR for 35 to 38 cycles of 15 s at 96°C, 20 s at 60°C, and 120 s at 72°C. Parental chromosome-specific histone modifications in the major-type promoter were analyzed by PCR using the primer set ChIP-F/ChIP-R for 30 cycles of 30 s at 95°C, 30 s at 58°C, and 30 s at 72°C. The PCR products were analyzed by direct sequencing with a BigDye Terminator cycle sequencing kit (PE Applied Biosystems) on an automated sequencer, the ABI Prism 3100 genetic analyzer (PE Applied Biosystems).

DNA methylation analysis. Isolated DNA was treated with sodium bisulfite using a CpGenome DNA modification kit (Chemicon International Inc., Temecula, CA) according to the manufacturer's protocol. Bisulfite-treated DNA samples were subjected to nested PCR amplification using the following first and second primer pairs, respectively, for each CGI; CGI1, Me1F/Me-1R and Me-1F′/Me-1R′; CGI2, Me-2F/Me-2R and Me-2F′/Me-2R′; and CGI3, Me-3F/Me-3R and Me-3F′/Me-3R′. After the first PCR using the first primer set, the products were used as templates for nested PCR using the second primer set. The nested PCR products were cloned into the TA cloning vector (Invitrogen), and at least 32 clones for each sample were sequenced.

ChIP. A chromatin immunoprecipitation (ChIP) assay was performed with a ChIP assay kit (Upstate Biotechnology, Lake Placid, NY) according to the manufacturer's protocol. In brief, the chromatin of cultured cells was prepared from ~1.0 × 10^6 cells and treated with formaldehyde to cross-link DNA to

TABLE 1. Primers used in this study

Function(s) and primer	Sequence (5′–3′)	Annealing temp (°C) (PCR cycle no.)[a]
Expression and imprinting analysis		
1aF[b]	CACGAAGTTTCCGCGCA	
1bF	GCGATCATTCGTCTCTGAGC	
1R[b]	AGTATCAGTATCAGACTGCATGTTG	
1cF	ATCGCCATCTACAGTTTCTG	
1cR	CAAGGTACAGAGCTAGGACG	
e2R	CTGGTTGGCTTCTTTGTTGTGG	
coR	TACGGATCTGCTCATCTTCG	
ChIP-F	TCACTTTAGAAACCGGGCA	
ChIP-R	AAACTCGGGCTTGCTCA	
Quantitative analysis		
Q-1bF	TCATTCGTCTCTGAGCGGCA	
Q-1bR	ATACGTGTTACATGCGCCAA	
Q-ChIP1F	TCACTTTAGAAACCGGGCA	
Q-ChIP1R	AAACTCGGGCTTGCTCA	
Q-ChIP2F	GATCATTCGTCTCTGAGC	
Q-ChIP2R	ATGCGGCAACATGCGCTGACA	
Hot-stop PCR and SSCP analysis		
ChIP2F-1	TCATTCGTCTCTGAGCGGCA	60 (32)
ChIP2R-1	TCTGGAGCCTAGAGGAGCG	
ChIP2F-2	AAGCGCGTGCTGGTTTGTA	60 (35)
ChIP2R-2	ATACGTGTTACATGCGCCAA	
DNA methylation analysis		
CGI1 1st		53 (35)
Me-1F	TGGGGTTTAATATTAAGTTTGA	
Me-1R	TTACATCTCTTAAATAAAACA	
CGI1 2nd		53 (35)
Me-1F′	TGGGGTTTAATATTAAGTTTGA	
Me-1R′	AAATCACCTATAACTCTCCTAC	
CGI2 1st		50 (40)
Me-2F	TGGAGTTTAGAGGAG	
Me-2R	AATAGTTATTTTAGTAAGGG	
CGI2 2nd		50 (10)
Me-2F′	TGGAGTTTAGAGGAG	
Me-2R′	TAAGTGAAGTAATATAGTT	
CGI3 1st		53 (40)
Me-3F	AAAGAAGGTTTGGAGAGATTATTT	
Me-3R	CAAACCAAAACTTACTATATTTAATTTAAAC	
CGI3 2nd		53 (10)
Me-3F′	AAGGTTTGGAGAGATTATTTTTGATT	
Me-3R′	TAATTTAAACTTAACACTATTAAATACC	

[a] For expression and imprinting analysis, the annealing temperature and PCR cycle number depend on the combination of primers used for each analysis. See details in Materials and Methods. For quantitative analysis, the PCR conditions were decided according to the manufacturer's protocol.
[b] Also used for quantitative analysis.

protein in situ, sonicated to an average size of 0.5 kb, and immunoprecipitated with antibodies. Antibodies against acetyl histone H3 (H3Ac; catalog no. 06-599), acetyl histone H4 (H4Ac; catalog no. 09-866), Lys4 dimethylated histone H3 (H3mK4; catalog no. 07-030), Lys9 trimethylated H3 (H3me3K9; catalog no. 07-212), and Lys27 trimethylated H3 (H3mK27; catalog no. 07-449) were obtained from Upstate Biotechnology. The monoclonal antibody against Lys9 dimethylated histone H3 (H3me2K9) was developed previously (26). Immunoprecipitated samples without antibodies or with rabbit immunoglobulin G precipitation were used as negative controls for precipitations with specific antibodies in each experiment.

Quantitative analysis of immunoprecipitated DNA by real-time PCR. Immunoprecipitated DNA and input DNA were analyzed by real-time PCR using the same protocol as that used for gene expression analysis. For DNA immunoprecipitated with H3Ac, H4Ac, and H3mK4 antibodies, the quantitative value of immunoprecipitated DNA in each CGI was normalized by dividing the average value of each CGI by that of the internal control, *Gapdh*. For DNA immunoprecipitated with H3me2K9 and H3me3K9 antibodies, the average value of *D13Mit55* was used instead of the value of *Gapdh*. Each normalized value of immunoprecipitated DNA was further divided by the normalized value of the corresponding input DNA. For the evaluation of DNA immunoprecipitated with H3mK27 antibody, the results were presented as a percentage of immunoprecipitation, calculated by dividing the average value of immunoprecipitated DNA by the average value of the corresponding input DNA. Each experiment was performed three times with independent chromatin extracts. The primers used for real-time PCR were primers Q-ChIP1F and Q-ChIP1R for CGI1 analysis and primers Q-ChIP2F and Q-ChIP2R for CGI2 analysis. The primers for *Gapdh* and *D13Mit55* have been described elsewhere (16).

Hot-stop PCR and SSCP analysis. Hot-stop PCR was performed for the analysis of allele-specific histone modifications as follows. After a number of PCR cycles sufficient to detect a product using primers ChIP2F-1 and ChIP2R-1, primer ChIP2R-1 labeled by [γ-^{32}P]ATP was added to the mixture, and then one cycle of PCR was performed. The PCR products were digested with the restriction endonuclease Hpy188I and electrophoresed in a 4% polyacrylamide gel. Single-strand conformation polymorphism (SSCP) analysis of PCR products was performed for allele-specific histone methylation in the presence of [γ-^{32}P]ATP-labeled primers ChIP2F-2 and ChIP2R-2. PCR products were resolved by electrophoresis in an MDE nondenaturing acrylamide gel (FMC BioProduct, Rockland, ME).

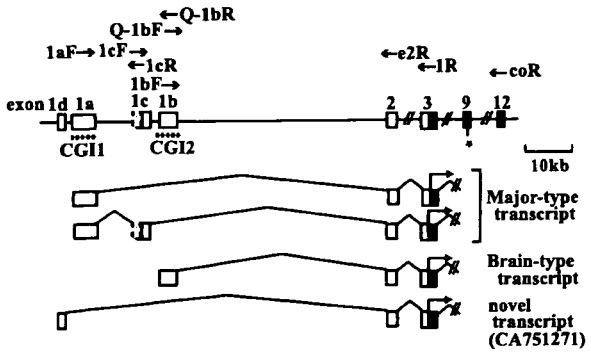

FIG. 1. Tissue-specific transcripts of *Grb10*. Filled boxes, open boxes, and shaded boxes represent protein-coding regions, 5′ untranslated regions, and extended exons 1c, respectively. The dashed lines indicate the CpG islands (CGI1 and CGI2) in the promoters. The primers used for RT-PCR are shown. The asterisk indicates the polymorphic site (G/A) between the C57BL/6 and PWK strains.

Primers. The primers used for the analysis are listed in Table 1.

RESULTS

Mouse *Grb10* has several tissue-specific promoters. Three different promoters of *Grb10* have previously been reported to initiate tissue-specific transcripts (Fig. 1). We first analyzed the expression of each transcript in E16 fetal tissues. The major-type transcript amplified by PCR using primers 1aF and e2R in exons 1a and 2, respectively, was detected in the fetal brain but was less detected in other tissues, while the brain type transcript amplified by primers 1bF and e2R in exons 1b and 2, respectively, was detected exclusively in the fetal brain (Fig. 2A). Another transcript which was previously reported to be brain specific in adult tissues (1) was examined in fetal tissues. PCR using primers 1cF and e2R in exons 1c and 2, respectively, showed that exon 1c was expressed not only in the fetal brain but also in the fetal liver and kidney (Fig. 2A). To assess whether exon 1c is an alternatively spliced exon of the major-type transcript with exon 1a, we performed PCR using primers 1aF and 1cR in exons 1a and 1c, respectively. The PCR product containing exons 1a and 1c was detected in the fetal tissues (Fig. 2A). Sequence analysis of the RT-PCR product revealed that exon 1c was extended 67 bp upstream of the previously published exon 1c with the consensus splicing site (Fig. 1). Any RT-PCR products with both exons 1a and 1b or both exons 1c and 1b were not found (data not shown). Furthermore, we identified another putative exon, 1d, located 1.2 kb upstream of exon 1a in the expressed sequence tag database (GenBank accession no. CA751271). The existence of the novel exon 1d was confirmed by RT-PCR in the embryonic liver but not in other tissues, including the brain (data not shown).

Expression of *Grb10* shifts from the major-type to the brain type transcript during brain development. To confirm whether the expression level of the brain type transcript changes during brain development, the major-type and brain type transcripts arising from exons 1a and 1b, respectively, were quantitatively analyzed at various developmental stages of the brain. Real-time PCR analysis showed that in the brain, the major-type transcript was highly expressed at E10 and decreased according to brain development, while expression of the brain type transcript was high in the perinatal period and gradually decreased thereafter (Fig. 2B). The result indicates that *Grb10* transcripts shift from the major type to the brain type during early brain development.

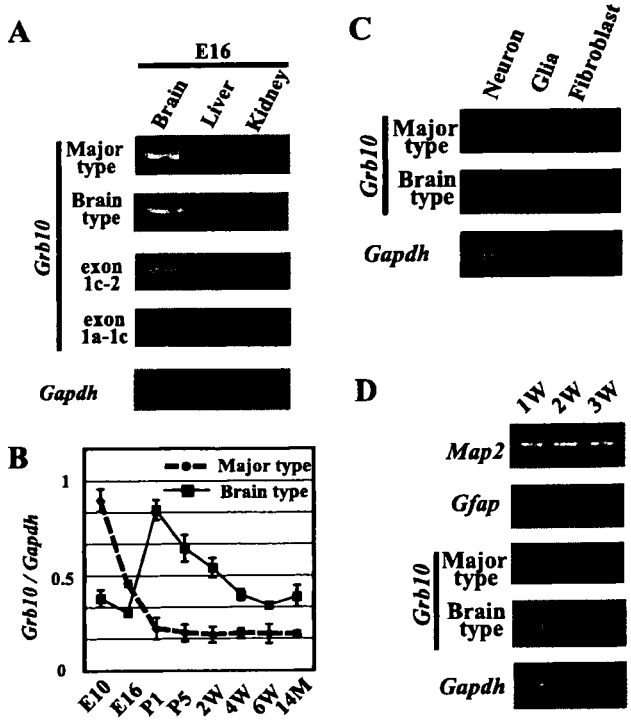

FIG. 2. Expression analysis of each transcript in embryonic tissues by RT-PCR. (A) Semiquantitative analysis of tissues from the E16 embryo. Exon 1c-2 and exon 1a-1c represent RT-PCR products amplified by primer sets 1cF/e2R and 1aF/1cR, respectively. The concentration of each cDNA was adjusted for *Gapdh* amplification as an internal control. (B) Quantitative evaluation of major-type and brain type transcripts in brain tissues from different developmental stages by real-time PCR. The relative amounts of major-type and brain type transcripts are shown. The relative amount of each transcript was calculated by normalizing each value with an internal control, *Gapdh*. Standard errors of the means are indicated by bars. (C) Expression analysis of major-type and brain type transcripts in the primary cell culture. (D) Evaluation of expression of marker genes and each *Grb10* transcript according to the culture period. 1w (1 week), 2w (2 weeks), and 3w (3 weeks) indicate the periods of neuron culture. P1, postnatal day 1; 14M, 14 months.

The brain-specific transcript is expressed in neurons but not in glial cells. Is the brain type transcript expressed exclusively in the brain restricted to the cell type? To know which type of brain cells, neurons or glial cells, express the brain type transcript, expression analysis of cultured neurons and glial cells was carried out. Prior to the analysis, we confirmed by immunostaining and RT-PCR with the brain precursors, neuronal and glial markers, that over 95% of the two cultured cell types were postmitotic neurons and astrocytes, respectively (data not shown). RT-PCR in cultured cells revealed that the major-type transcript was expressed in all cultured brain cells but that the brain type transcript was expressed only in neurons (Fig. 2C). We next tried to investigate whether these transcripts in the brain were associated with the maturation of

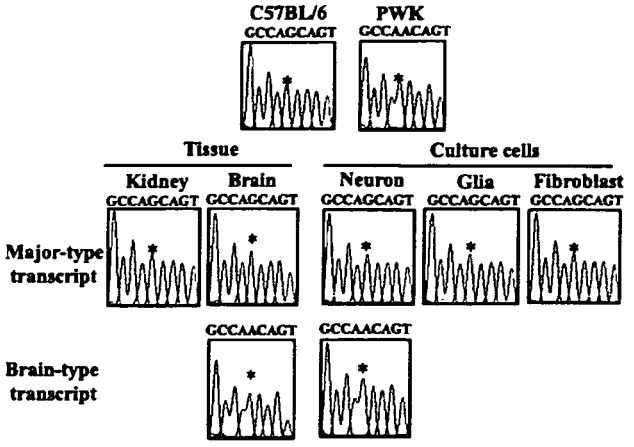

FIG. 3. Imprinting analysis of promoter-specific expression of *Grb10* by sequence chromatograms. Upper panels show the chromatograms of the genomic PCR products from each strain. Middle and lower panels show the chromatograms of the RT-PCR products from tissues and cultured cells of the F_1 hybrid, in which alleles were distinguished by the single-nucleotide (G/A) polymorphism (*) at exon 9.

neurons. Neurons were cultured for 1, 2, and 3 weeks, and semiquantitative RT-PCR was carried out. Before expression analysis of *Grb10*, the status of cell proliferation and differentiation by long culture was evaluated by primers for *Map2* as a marker for neurons and *Gfap* as a marker for astrocytes under the normalization of cDNA concentration to *Gapdh* (Fig. 2D). The expression of *Map2* never changed in 3-week-cultured cells, while that of *Gfap* was detected in the cells cultured for 3 weeks. In these long-culture cells, the brain type transcript was continuously expressed during culture periods, while the major-type transcript was less expressed than the brain type transcript. These results suggest that both types of transcripts are expressed in neurons and that the switching of the promoter from the major type to the brain type is observed during long culture periods.

Promoter-specific paternal expression of *Grb10* in the brain. To investigate the imprinted expression of *Grb10*, we first examined parental expression of the major-type and the brain type transcripts in the brain and kidney from F_1 hybrid mice by direct sequencing of the RT-PCR product. A polymorphic site (G/A) in exon 9 between the C57BL/6 and PWK strains was used to determine the paternal allele (Fig. 1). As previously reported by Hikichi et al. (17), the major-type transcript was expressed exclusively from the maternal allele in the kidney and brain, while the brain type transcript was expressed from the paternal allele only in the brain (Fig. 3). We next examined promoter-specific imprinting in neurons, glial cells, and fibroblasts. Expression of the major-type transcript originated exclusively from the maternal allele in all cultured cells, but that of the brain type transcript detected only in neurons originated from the paternal allele (Fig. 3). Thus, predominant paternal *Grb10* expression in the brain, as previously described, can be explained by a combination of paternally expressed brain type transcript in neurons and maternally expressed major-type transcript in all cells.

Differentially methylated CGI2 is maintained in cultured neurons and glial cells. As we found that the brain type transcript was initiated from exon 1b of the paternal allele only in neurons, we analyzed the methylation status of the brain type promoter in neurons and glial cells by the bisulfite method. As shown in Fig. 4A, three promoters are located within different CGIs: exon 1a in CGI1, exon 1b in CGI2, and exon 1c in the "weaker" CpG island, CGI3. The parental origin of the methylated allele was identified by polymorphic sites in F_1 hybrids between the C57BL/6 and PWK strains. The methylation analysis of CGI2 showed that the differential methylation established in the germ cells (1, 17) was maintained in neurons and glial cells (Fig. 4B). That in other CpG islands, CGI1 and CGI3, revealed biallelic hypomethylation and hypermethylation, respectively. CGI1 and CGI3 did not show any differential methylation in the cells, although CGI3 was reported to be a putative differentially methylated region in the mouse brain with uniparental disomy for chromosome 11 (1) The methylation status in CGIs, except CGI3, in cultured cells was consistent with that previously reported for tissues (1, 17).

Parental chromosome-specific histone modifications in CGI2 correlate with allele-specific expression of the brain type transcript in neurons. Parental origin-specific histone modifications are reported to represent the determinant of epigenetic features as well as DNA methylation. Using specific antibodies against acetylated histone H3 (H3Ac), acetylated histone H4 (H4Ac), dimethylated Lys4 histone H3 (H3mK4), and di- and trimethylated Lys9 histone H3 (H3me2K9 and H3me3K9), we performed a ChIP assay with cultured cells. After evaluation of ChIP DNA by allele-specific histone modifications in the *Lit1* promoter region as a control (16), histone modifications in CGI1, CGI2, and CGI3 were analyzed by real-time PCR to quantify their precipitated chromatins in these CGIs. To normalize each value, *Gapdh* and *D13Mit55* were used as internal control sequences, where acetylated and methylated histones were known to be biallelically immunoprecipitated, depending on the corresponding antibodies. In CGI2, where the maternal allele-specific DNA methylation was established in the oocyte, H3Ac, H4Ac, H3mK4, and H3me3K9 were clearly immunoprecipitated in neurons, while in glial cells and fibroblasts, although H3mK4 and H3me3K9 were well immunoprecipitated, H3Ac and H4Ac were less precipitated (Fig. 5A). The results obtained with the antibody against H3me2K9 (data not shown) were similar to those obtained with the antibody against H3me3K9.

To elucidate the parental chromosome-specific histone modifications in CGI2 in neurons, hot-stop PCR was performed (15, 32). The restriction endonuclease Hpy188I was used to recognize the polymorphic site in CGI2. For each of the precipitated samples, the ratio of the paternal to maternal band intensities was determined. These ratios were corrected for the paternal-to-maternal ratios in the input chromatin, because the maternal and paternal alleles were not equally represented in the input chromatin. One of the parental alleles is possibly more sensitive to sonication in these regions because of relaxed chromatin (12, 16, 39). The result revealed that histones H3 and H4 were hyperacetylated and that H3K4 was hypermethylated predominantly on the paternal chromosome (Fig. 5B). To investigate allele-specific histone trimethylation of H3K9 in neurons and fibroblasts, SSCP analysis of PCR products was also performed. In

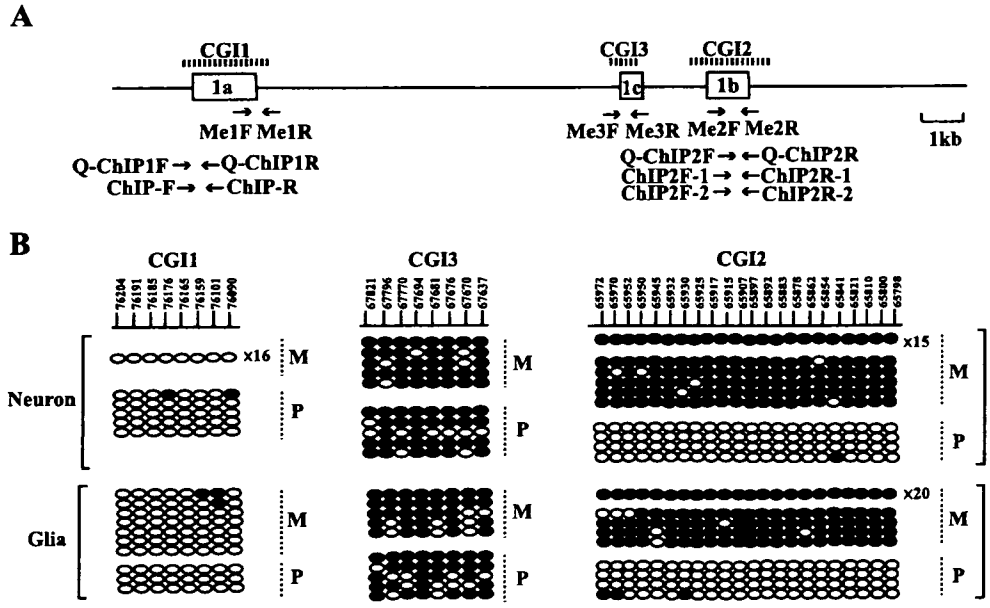

FIG. 4. Methylation status of CpG islands in neurons and glial cells. (A) Schematic structure of CpG islands. The dashed lines indicate the registered regions of CGI1, CGI2, and CGI3 (1, 17). Open boxes and arrows represent exons and primers used for methylation analysis and ChIP analysis, respectively. (B) Allele-specific DNA methylation analysis of cultured cells by bisulfite PCR and sequencing. Numbers on the line in the upper panel represent nucleotide positions, given according to GenBank accession no. AL663087. Each line shows an individual clone, and each oval represents a CpG nucleoside; the filled and open ovals indicate hypermethylated and hypomethylated CpGs, respectively. The numbers with "×" given at the right end of the clone lines represent the number of individual clones that show the same pattern of DNA methylation. Parental alleles (M, maternal; P, paternal) are distinguished by DNA polymorphisms between the C57BL/6 and PWK strains.

neurons and fibroblasts, H3K9 was hypermethylated on the maternal chromosome (Fig. 5C).

Parental chromosome-specific methylation of histone H3K27 but not H3K9 in CGI1 correlates with allele-specific expression of the major-type transcript. Histone modifications in CGI1, where CpGs were biallelically hypomethylated in tissues and cultured cells, were next analyzed. In CGI1, H3Ac, H4Ac, and H3mK4 were clearly precipitated in glial cells and fibroblasts, while the precipitations were not observed in neurons (Fig. 5A). H3me3K9 and H3me2K9 in CGI1 were not precipitated in neurons and glial cells (Fig. 5A; data not shown). The maternal chromosome-specific histone H3/H4 acetylation and H3K4 methylation in CGI1 were detected in glial cells and fibroblasts (Fig. 5D). We further analyzed histone H3K27 trimethylation, which is directly regulated by the PcG proteins, because imprinted expression of the major-type *Grb10* transcript was reported to be relaxed in the knockout embryos of the PcG gene, *Eed* (24). In neurons and fibroblasts, H3mK27 was clearly precipitated in CGI1 but not in CGI2 (Fig. 6A). The paternal chromosome-specific methylation of H3K27 was observed in fibroblasts, but a significant allelic difference was not detected in neurons (Fig. 6B). These data suggest that the paternally null expression of the major-type transcript in fibroblasts correlates with paternal chromosome-specific methylation of H3K27 in CGI1. In CGI3, histones H3 and H4 were hypoacetylated and H3K4 was hypomethylated (data not shown). We could not detect significant differences in histone acetylation and methylation in CGI3 between cultured cells.

DISCUSSION

It has been known that mouse *Grb10* shows reciprocal imprinting depending on the tissue-specific promoters. In most tissues, *Grb10* is expressed exclusively from the maternal allele, whereas in the brain, it is expressed predominantly from the paternal allele (1, 17). Such reciprocal imprinting of *Grb10* in a tissue-specific and promoter-specific manner is a good model to elucidate how promoter-specific imprinting is epigenetically controlled in tissues. In this study, we have developed a cell culture system with which cell-type-specific imprinting of *Grb10* can be characterized in the mouse brain. We demonstrated that promoter-specific and developmental stage-specific imprinting of *Grb10* expression in the brain is associated with parental allele-specific epigenetic modifications in brain cell lineages.

Two previous reports described that reciprocal imprinting of *Grb10* occurs in a tissue-specific and promoter-specific manner (1, 17). Our studies with cultured cortical cells revealed that the brain type transcript containing exon 1b was expressed in neurons but not in glial cells, while the major-type transcript containing exon 1a was expressed in all cultured cells, including neurons (Fig. 2C). These findings indicate that the brain-specific promoter actually implies the neuron-specific promoter and that the major-type promoter works as the common promoter in all tissues. Imprinting analysis of these transcripts clearly showed that the brain type transcript is expressed exclusively from the paternal allele and the major-type transcript is expressed exclusively from the maternal allele (Fig. 3). These

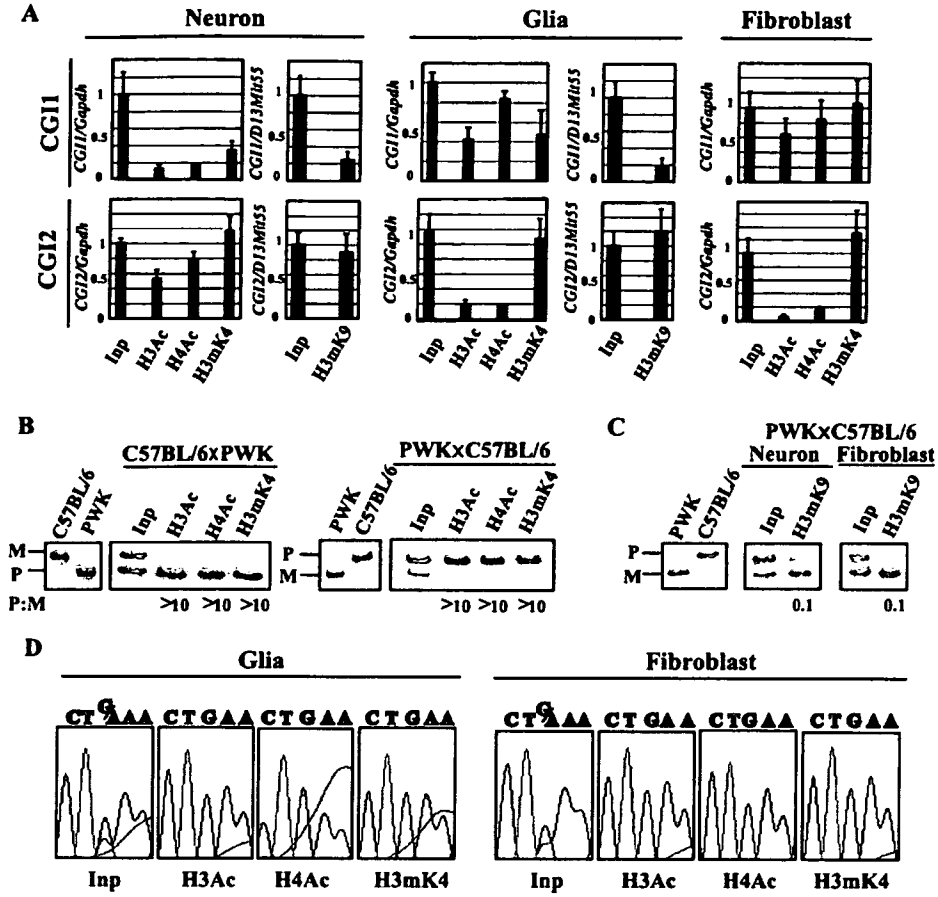

FIG. 5. Histone modification analysis of the *Grb10* promoter in cultured cells. (A) Quantitative analysis of immunoprecipitated DNA by real-time PCR. Quantitative values of precipitated DNA in CGI1 and CGI2 were normalized by dividing the average value of each CGI by the average value of *Gapdh* or *D13Mit55*. Standard errors of the means are indicated by bars. (B) Allele-specific histone modifications in CGI2 in neurons by hot-stop PCR. Digested PCR products of C57BL/6 and PWK genomic DNA are shown as homozygous controls in the first two lanes. M and P represent the products from the maternal allele and the paternal allele, respectively. The ratio of the paternal to maternal (P:M) band intensities, corrected by the ratio in input chromatin (Inp), is indicated below each lane. (C) Allele-specific histone H3K9 methylation in CGI2 by SSCP. PCR products of C57BL/6 and PWK genomic DNA were shown as controls in the first two lanes. (D) Allele-specific histone modifications in CGI1 by sequence chromatograms. Glial cells and fibroblasts derived from F_1 hybrids [(C57BL/6 × PWK)F_1] were used for analysis. The single-nucleotide (G/A) polymorphism is detected in the input sample (Inp); "G" originated from the maternal allele and "A" from the paternal allele.

results in vitro can explain the previous data that the brain type transcript was not detected in whole embryo at E9.5 (17), when neurogenesis has not yet occurred. In addition, our data on *Grb10* expression, i.e., brain development-dependent switching from the major-type to the brain type transcript, can also support the previous report that *Grb10* is expressed predominantly from the paternal allele in the adult brain (17), which consists of neurons and glial cells.

In our expression analysis, we detected both brain type and major-type transcripts in cultured neurons (Fig. 2B). Recently, it was reported that the *Pcdh* (protocadherin) gene was monoallelically expressed in individual neurons (10). The *Pcdh* gene family (*Pcdha*, *Pcdhb*, and *Pcdhc*) has variable exons and alternative splice forms. Esumi et al. analyzed the expression of transcripts in the variable exons of *Pcdha* by using a single-cell RT-PCR approach for the determination of the allelic origin for each variable exon at the individual cell level (10). The individual cells showed monoallelic expression for each variable exon. In our analysis of *Grb10*, the discrepancy between the modifications in CGI1 and the expression of the major-type transcript in neurons was recognized. Similar to a monoallelic expression pattern of variable *Pcdha* exons in individual neurons, the discrepancy may be explained by the existence of two different cell populations in cultured neurons, each of which expresses either the major-type or the brain type transcript exclusively. As shown in Fig. 2D, the brain type transcript was obviously highly expressed compared to the major-type transcript during long culture periods. The larger population of cells with the brain type transcript may affect the result of histone modifications more than the smaller population of cells with the major-type transcript.

It has been reported that histone modifications and DNA methylation are not synchronized as a transcriptionally active/silent signal in some imprinted genes, such as *NDN*, *Gnas*, and

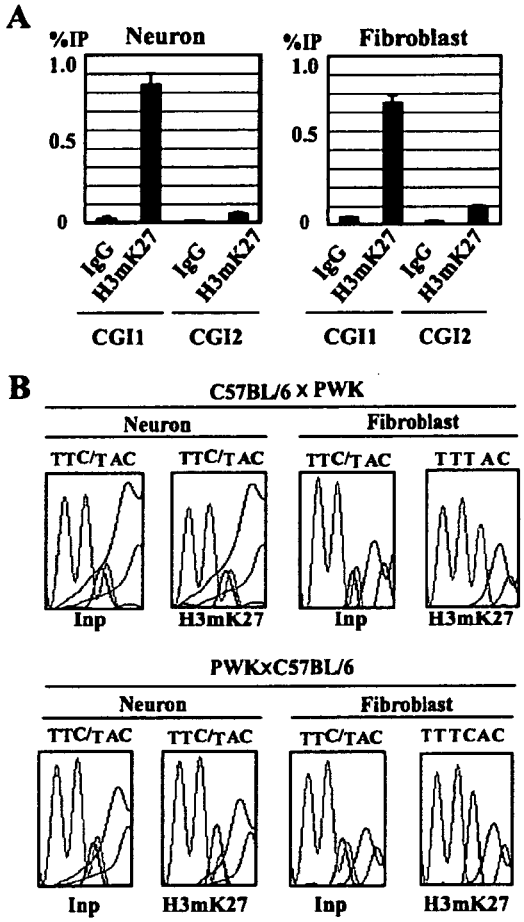

FIG. 6. Histone H3K27 methylation analysis of CGI1 and CGI2 in cultured cells. (A) Quantitative analysis of immunoprecipitated DNA by real-time PCR. The percentage of immunoprecipitation (IP) was calculated by dividing the quantitative value of precipitated DNA by that of the corresponding input DNA. Standard errors of the means are indicated by bars. (B) Allele-specific histone modifications in CGI1 by sequence chromatograms. Neurons and fibroblasts derived from F_1 hybrids (C57BL/6 × PWK; PWK × C57BL/6) were used for analysis. The single-nucleotide (C/T) polymorphism is detected in the input sample (Inp); "C" originated from the C57BL/6 allele and "T" from the PWK allele. IgG, immunoglobulin G.

Igf2r (21, 22, 23, 33, 35). Our data also showed an epigenetically unsynchronized active/silent signal between DNA methylation and histone modifications in *Grb10* (Fig. 7). In this study, we showed that the brain type transcript is expressed in neurons but not in glial cells (Fig. 2C), where both differential methylation in CGI2 and biallelic hypomethylation in CGI1 were maintained regardless of expression (Fig. 4B). The result that allele-specific DNA methylation is not sufficient to direct imprinted expression in brain cells implies that other epigenetic modifications may affect cell lineage-specific imprinting.

In our analysis of histone modifications, histone acetylation status correlated with the expression status of the major-type transcript in glial cells and fibroblasts and the brain type transcript in neurons (Fig. 7). Such histone acetylation status in *Grb10* expression is consistent with the findings that allele-specific histone acetylation was associated with allelic gene expression in the imprinted gene, *NDN* (21). Histone acetylation offers the best example of a direct link between tissue-specific gene expression and histone modifications.

Unlike that of histone acetylation, the status of histone methylation has been implicated as an early event for chromatin conformations. Methylation of histones H3K4 and H3K9 is associated with active chromatin and silent chromatin, respectively. According to our results, allele-specific H3K4 and H3K9 methylation in CGI1 and CGI2 did not correlate with allele-specific gene expression in each cultured cell. In glial cells, H3K4 in CGI2 was hypermethylated in the paternal chromosome, which was silent with no brain type transcript. It seems that H3mK4 is maintained during differentiation as an imprint mark with H3mK9 but is not related to promoter activity (28), although histone modifications in oocytes remain unknown. In CGI1, H3me2K9 and H3me3K9 were hypomethylated in both parental chromosomes independent of the expression of the major-type transcript in cultured cells. It is likely that H3K9 methylation in germ cells is maintained as a stable and heritable imprint mark but may not be secondarily acquired during development.

Then, how is maternal chromosome-specific expression of the major-type transcript regulated without differential DNA methylation in CGI1? The PcG protein Eed complex is known to be a part of a memory system that maintains repression of

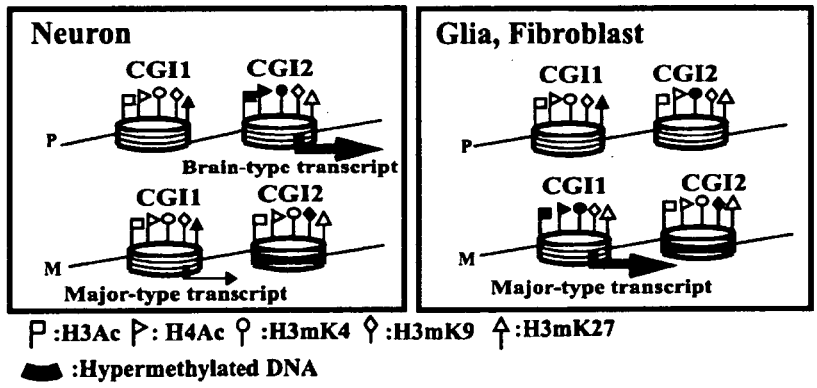

FIG. 7. Summary of epigenetic modifications across promoter regions of *Grb10*. M and P represent maternal and paternal chromosomes, respectively. Large and small arrows indicate expression levels. The nucleosome model shows DNA wrapping around a histone octamer with some histone modifications. White and black flags represent hypoacetylated/hypomethylated and hyperacetylated/hypermethylated statuses, respectively.

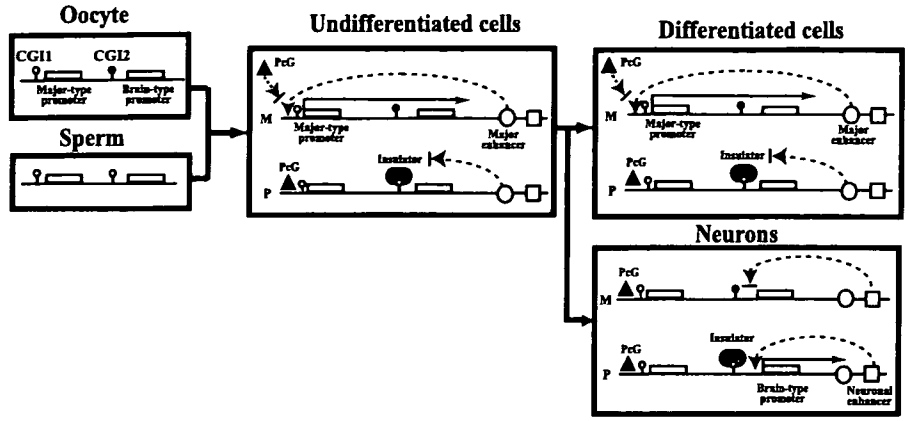

FIG. 8. Working models for tissue-specific reciprocal imprinting of *Grb10*. The previous enhancer/insulator model by Hikichi et al. was modified based on the analysis of DNA methylation and histone modifications mediated by the PcG complex containing Eed (17). Tissue-specific imprinting of *Grb10* implies neuron-specific imprinting that is different from imprinting in other undifferentiated and differentiated cells. Black and white lollipops indicate hypermethylated and hypomethylated DNA, respectively. Circles and squares indicate putative major enhancer and neuronal enhancer, respectively, which accelerate *Grb10* expression from the major-type promoter and the brain type promoter, respectively. The PcG complex containing Eed is represented by a triangle. CTCF is thought to be a putative insulator (gray oval). M, maternal; P, paternal.

the imprinted X chromosome (36) and silencing of some imprinted genes (24, 33). *Grb10* is reported to be one of the imprinted genes that are regulated by the PcG protein Eed complex. Interestingly, in $Eed^{-/-}$ embryos, the major-type transcript was biallelically expressed without major alteration of allelic DNA methylation (24). The Eed/Ezh2 PcG complex possesses histone methyltransferase activity on H3K27 (5, 8, 25) and interacts with histone deacetylases (34). Methylation of H3K27 is a repressive epigenetic mark regulated by the SET domain containing Ezh2/Eed complex (5, 8, 20, 25). In our analysis, H3mK27 was clearly precipitated in neurons and fibroblasts in CGI1 but not in CGI2 (Fig. 6A). The paternal chromosome-specific methylation of H3K27 in CGI1 was observed in fibroblasts but not in neurons (Fig. 6B). These data indicate that the Eed PcG complex can biallelically interact on CGI1 as a *trans*-acting factor in neurons but paternally in other cells. In the absence of DNA methylation in CGI1, PcG complexes may mediate a nonpermissive chromatin state for transcription, leading to repressive histone modifications. Interestingly, other genes, *Cdkn1c* and *Ascl2*, imprinting of which was reported to be regulated by Eed (24), show tissue-specific imprinting, and their imprinted expression in trophoblasts is associated with repressive histone H3K27 methylation rather than DNA methylation (22, 33).

Figure 7 shows the summary of our data. In CGI2, DNA methylation in a gametically methylated CpG island on the maternal allele was maintained throughout development. Allelic methylation of H3K4 and H3K9 associated with gametic DNA methylation was also stable as an epigenetic mark, independent of *Grb10* expression. Histone acetylation status was correlated with the expression status of the brain type transcript: histones H3 and H4 were paternally acetylated only in neurons, where the brain type transcript was paternally expressed. H3K27 was not methylated biallelically. In CGI1, biallelic DNA hypomethylation and biallelic hypomethylation of H3K9 were observed. Acetylation of histones H3 and H4 and methylation of H3K4 and H3K27 were allelically detected, corresponding to the allelic expression of the major-type transcript, although the discordance in histone modifications and expression in neurons was detected, probably depending on maturation of neurons. Methylation of H3K9 and H3K27 is thought to be a repressive chromatin marker, but it is not completely clear whether PcG-mediated silencing involves methylation of H3K9 synchronized with H3mK27 in all PcG target genes. We did not observe coexistence of H3mK27 and H3mK9 in both CGI1 and CGI2 of *Grb10*. Umlauf et al. also reported discordance between localizations of H3mK27 and H3mK9 in some imprinted genes in the *Kcnq1* domain (33). Further work should determine how histone modifications, especially methylation of H3K9 and H3K27, are coordinated or uncoordinated as epigenetic determinants in tissue-specific imprinting.

These data about epigenetic modifications analyzed at the cell level, in addition to the evidence for $Dnmt3L^{m-/-}$ and $Eed^{-/-}$ embryos, lead to a working model for tissue-specific reciprocal imprinting of *Grb10* (Fig. 8). The previous model by Hikichi et al. (17) was modified in our model based on the data of DNA methylation and repressive histone modifications mediated by the PcG complex in brain cell lineages. In undifferentiated cells, a DNA methylation-sensitive insulator, CTCF, binds to the paternal CGI2 and blocks the paternal activity of the downstream major enhancer, resulting in silent expression of the major-type transcript on the paternal allele. On the maternal allele, the major enhancer works on the major-type promoter to recruit transcription factors. In CGI1, the Eed/Ezh2 PcG complex binds on the paternal allele, whereas it competes with transcription factors on the maternal allele. The Eed/Ezh2 PcG complex methylates H3K27 and interacts with histone deacetylases, leading to silencing of the chromatin on the paternal CGI1. In $Dnmt3L^{m-/-}$ embryos, biallelic hypomethylation in CGI2 makes CTCF bind biallelically on CGI2, resulting in null expression of the major-type transcript, regardless of the PcG complex. In $Eed^{-/-}$ embryos, the silent state on the paternal CGI1 regulated by the Eed PcG complex

is released to the biallelically active state without major alteration of DNA methylation in maternal CGI2. In neurons, the other molecular mechanism of imprinting works in a promoter-specific manner, different from that in other differentiated cells. During neurogenesis, expression of *Grb10* shifts from the major-type to the brain type transcript by switching from the major-type promoter to the brain type promoter. The neuronal enhancer instead of the major enhancer may work on the brain type promoter, depending on DNA methylation in CGI2. The maternally active major-type promoter becomes silent without transcription factors, and consequently, the Eed/Ezh2 PcG complex binds to make the chromatin structure silent. This implies that the PcG complex is necessary to maintain cell-type-specific imprinting. It remains unknown how neuron-specific imprinting is regulated by DNA methylation and/or histone modifications mediated by the PcG complex, because *Dnmt3L*$^{m-/-}$ and *Eed*$^{-/-}$ embryos are lethal by E10.5 (4, 14) and E8.5 (11), respectively, just before neurogenesis.

As far as we know, this is the first report of an epigenetic analysis of cultured cells where DNA methylation and chromatin remodeling by PcG proteins establish and maintain cell-type-specific imprinting at one gene locus. Although allelic DNA methylation established in the gamete contributes primarily to tissue-specific imprinting, tissue-specific *Grb10* imprinting is directly regulated by the repressive chromatin mediated by the PcG complex during development. Our analysis of promoter-specific and cell-type-specific imprinting of *Grb10* gives an important clue for understanding the mechanism of tissue-specific imprinting.

ACKNOWLEDGMENTS

We thank F. Ishino for providing information about genomic sequences of *Grb10* promoter regions.

T.K. was supported in part by a Grant-in-Aid for Scientific Research (C) and a Grant-in-Aid on Priority Areas (Molecular Brain Science) from the Ministry of Education, Culture, Sports, Science and Technology of Japan.

REFERENCES

1. **Arnaud, P., D. Monk, M. P. Hichins, E. Gordon, W. Dean, C. Beechey, J. Peters, W. Craigen, M. Preece, P. Stanier, G. E. Moore, and G. Kelsey.** 2003. Conserved methylation imprints in the human and mouse GRB10 genes with divergent allelic expression suggests differential reading of the same mark. Hum. Mol. Genet. **12**:1005–1019.
2. **Arnaud, P., K. Hata, M. Kaneda, E. Li, H. Sasaki, R. Feil, and G. Kelsey.** 2006. Stochastic imprinting in the progeny of Dnmt3L−/− females. Hum. Mol. Genet. **15**:589–598.
3. **Bantignies, F., and G. Cavalli.** 2006. Cellular memory and dynamic regulation of Polycomb group proteins. Curr. Opin. Cell Biol. **18**:1–9.
4. **Bourc'his, D., G. L. Xu, C. S. Lin, B. Bollman, and T. H. Bester.** 2001. Dnmt3L and the establishment of maternal genomic imprints. Science **294**: 2536–2539.
5. **Cao, R., L. Wang, H. Wang, L. Xia, H. Erdjument-Bromage, P. Tempst, R. S. Jones, and Y. Zhang.** 2002. Role of histone H3 lysine 27 methylation in Polycomb-group silencing. Science **298**:1039–1043.
6. **Cattanach, B. M., and C. V. Beechey.** 1990. Autosomal and X-chromosome imprinting. Dev. Suppl. **1990**:63–72.
7. **Constancia, M., B. Pickard, G. Kelsey, and W. Reik.** 1988. Imprinting mechanisms. Genome Res. **8**:881–900.
8. **Czermin, B., R. Melfi, D. McCabe, V. Seitz, A. Imhof, and V. Pirrotta.** 2002. Drosophila enhancer of Zeste/ESC complexes have a histone H3 methyltransferase activity that marks chromosomal Polycomb sites. Cell **111**:185–196.
9. **Davies, W., A. R. Isles, and L. S. Wilkinson.** 2005. Imprinted gene expression in the brain. Neurosci. Biobehav. Rev. **29**:421–430.
10. **Esumi, S., N. Kakazu, Y. Taguchi, T. Hirayama, A. Sasaki, T. Hirabayashi, T. Koide, T. Kitsukawa, S. Hamada, and T. Yagi.** 2005. Monoallelic yet combinatorial expression of variable exons of the protocadherin-α gene cluster in single neurons. Nat. Genet. **37**:171–176.
11. **Faust, C., A. Schumacher, B. Holdener, and T. Magnuson.** 1995. The eed mutation disrupts anterior mesoderm production in mice. Development **121**: 273–285.
12. **Fournier, C., Y. Goto, E. Ballestar, K. Delaval, A. M. Hever, M. Esteller, and R. Feil.** 2002. Allele-specific histone lysine methylation marks regulatory regions at imprinted mouse genes. EMBO J. **21**:6560–6570.
13. **Gregory, R. I., T. E. Randall, C. A. Johnson, S. Khosla, I. Hatada, L. P. O'Neill, B. M. Turner, and R. Feil.** 2001. DNA methylation is linked to deacethylation of histone H3, but not H4, on the imprinted genes *Snrpn* and *U2af1-rs1*. Mol. Cell. Biol. **21**:5426–5436.
14. **Hata, K., M. Okano, H. Lei, and E. Li.** 2002. Dnmt3L cooperates with the Dnmt3 family of de novo DNA methyltransferases to establish maternal imprints in mice. Development **129**:1983–1993.
15. **Higashimoto, K., H. Soejima, H. Yatsuki, K. Joh, M. Uchiyama, Y. Obata, R. Ono, Y. Wang, Z. Xin, X. Zhu, S. Masuko, F. Ishino, I. Hatada, Y. Jinno, T. Iwasaka, T. Katsuki, and T. Mukai.** 2002. Characterization and imprinting status of *OBPH1/Obph1* gene: implications for an extended imprinting domain in human and mouse. Genomics **80**:575–584.
16. **Higashimoto, K., T. Urano, K. Sugiura, H. Yatsuki, K. Joh, W. Zhao, M. Iwakawa, H. Ohashi, M. Oshimura, N. Niikawa, T. Mukai, and H. Soejima.** 2003. Loss of CpG methylation is strongly correlated with loss of histone H3 lysine 9 methylation at DMR-LIT1 in patients with Beckwith-Wiedemann syndrome. Am. J. Hum. Genet. **73**:948–956.
17. **Hikichi, T., T. Kohda, T. Kaneko-Ishino, and F. Ishino.** 2003. Imprinting regulation of the murine *Meg1/Grb10* and human *GRB10* genes; roles of brain-specific promoters and mouse-specific CTCF-binding sites. Nucleic Acids Res. **31**:1398–1406.
18. **Kaneda, M., M. Okano, K. Hata, T. Sado, N. Tsujimoto, E. Li, and H. Sasaki.** 2004. Essential role for de novo DNA methyltransferase Dnmt3a in paternal and maternal imprinting. Nature **429**:900–903.
19. **Kishino, T.** 2006. Imprinting in neurons. Cytogenet. Genome Res. **113**:209–214.
20. **Kuzmichev, A., K. Nishioka, H. Erdjument-Bromage, P. Tempst, and D. Reinberg.** 2002. Histone methyltransferase activity associated with a human multiprotein complex containing the Enhancer of Zeste protein. Genes Dev. **16**:2893–2905.
21. **Lau, J. C., M. L. Hanel, and R. Wevrick.** 2004. Tissue-specific and imprinted epigenetic modifications of the human *NDN* gene. Nucleic Acids Res. **32**: 3376–3382.
22. **Lewis, A., K. Mitsuya, D. Umlauf, P. Smith, W. Dean, J. Walter, M. Higgins, R. Feil, and W. Reik.** 2004. Imprinting on distal chromosome 7 in the placenta involves repressive histone methylation independent of DNA methylation. Nat. Genet. **36**:1291–1295.
23. **Li, T., T. H. Vu, G. A. Ulaner, Y. Yang, J. F. Hu, and A. R. Hoffman.** 2004. Activating and silencing histone modifications from independent allelic switch regions in the imprinted *Gnas* gene. Hum. Mol. Genet. **13**:741–750.
24. **Mager, J., N. D. Montgomery, F. P. de Villena, and T. Magnuson.** 2003. Genome imprinting regulated by the mouse Polycomb group protein Eed. Nat. Genet. **33**:502–507.
25. **Muller, J., C. M. Hart, N. J. Francis, M. L. Vargas, A. Sengupta, B. Wild, E. L. Miller, M. B. O'Connor, R. E. Kingston, and J. A. Simon.** 2002. Histone methyltransferase activity of a Drosophila Polycomb group repressor complex. Cell **111**:197–208.
26. **Nakagawachi, T., H. Soejima, T. Urano, W. Zhao, K. Higashimoto, Y. Satoh, S. Matsukura, S. Kudo, Y. Kitajima, H. Harada, K. Furukawa, H. Matsuzaki, M. Emi, Y. Nakabeppu, K. Miyazaki, M. Sekiguchi, and T. Mukai.** 2003. Silencing effect of CpG island hypermethylation and histone modifications on O6-methylguanine-DNA methyltransferase (*MGMT*) gene expression in human cancer. Oncogene **22**:8835–8844.
27. **Pirrotta, V.** 1995. Chromatin complexes regulating gene expression in Drosophila. Curr. Opin. Genet. Dev. **5**:466–472.
28. **Rougeulle, C., P. Navarro, and P. Avner.** 2003. Promoter-restricted H3 Lys 4 di-methylation is an epigenetic mark for monoallelic expression. Hum. Mol. Genet. **12**:3343–3348.
29. **Saitoh, S., and T. Wada.** 2000. Parent-of-origin specific histone acetylation and reactivation of a key imprinted gene locus in Prader-Willi syndrome. Am. J. Hum. Genet. **66**:1958–1962.
30. **Surani, M. A., S. C. Barton, and M. L. Norris.** 1984. Development of reconstituted mouse eggs suggests imprinting of the genome during gametogenesis. Nature **308**:548–550.
31. **Tilghman, S. M.** 1999. The sins of the fathers and mothers: genomic imprinting in mammalian development. Cell **96**:185–193.
32. **Uejima, H., M. P. Lee, H. Cui, and A. P. Feinberg.** 2000. Hot-stop PCR: a simple and general assay for linear quantitation of allele ratios. Nat. Genet. **25**:375–376.
33. **Umlauf, D., Y. Goto, R. Cao, F. Cerqueira, A. Wagschal, Y. Zhang, and R. Feil.** 2004. Imprinting along the *Kcnq1* domain on mouse chromosome 7 involves repressive histone methylation and recruitment of Polycomb group complexes. Nat. Genet. **36**:1296–1300.
34. **van der Vlag, J., and A. P. Otte.** 1999. Transcriptional repression mediated by the human polycomb-group protein EED involves histone deacetylation. Nat. Genet. **23**:474–478.
35. **Vu, T. H., T. Li, and A. R. Hoffman.** 2004. Promoter-restricted histone code,

not the differentially methylated DNA regions or antisense transcripts, marks the imprinting status of *IGF2R* in human and mouse. Hum. Mol. Genet. 13:2233–2245.

36. **Wang, J., J. Mager, Y. Chen, E. Schneider, J. C. Cross, A. Nagy, and T. Magnuson.** 2001. Imprinted X inactivation maintained by a mouse Polycomb group gene. Nat. Genet. 28:371–375.
37. **Wang, Y., K. Joh, S. Masuko, H. Yatsuki, H. Soejima, A. Nabetani, C. V. Beechey, S. Okinami, and T. Mukai.** 2004. The mouse *Murr1* gene is imprinted in the adult brain, presumably due to transcriptional interference by the antisense-oriented *U2af1-rs1* gene. Mol. Cell. Biol. 124:270–279.
38. **Yamasaki, K., K. Joh, T. Ohta, H. Masuzaki, T. Ishimaru, T. Mukai, N. Niikawa, M. Ogawa, J. Wagstaff, and T. Kishino.** 2003. Neurons but not glial cells show reciprocal imprinting of sense and antisense transcripts of *Ube3a*. Hum. Mol. Genet. 12:837–847.
39. **Yamasaki, Y., T. Kayashima, H. Soejima, A. Kinoshita, K. Yoshiura, N. Matsumoto, T. Ohta, T. Urano, H. Masuzaki, T. Ishimaru, T. Mukai, N. Niikawa, and T. Kishino.** 2005. Neuron-specific relaxation of *Igf2r* imprinting is associated with neuron-specific histone modifications and lack of its antisense transcript *Air*. Hum. Mol. Genet. 14:2511–2520.
40. **Yang, Y., T. Li, T. H. Vu, G. A. Ulaner, J. F. Hu, and A. R. Hoffman.** 2003. The histone code regulating expression of the imprinted mouse *Igf2r* gene. Endocrinology 144:5658–5670.

J Hum Genet (2007) 52:334–341
DOI 10.1007/s10038-007-0116-7

ORIGINAL ARTICLE

Paroxysmal kinesigenic choreoathetosis (PKC): confirmation of linkage to 16p11-q21, but unsuccessful detection of mutations among 157 genes at the PKC-critical region in seven PKC families

Taeko Kikuchi · Masayo Nomura · Hiroaki Tomita · Naoki Harada · Kazuaki Kanai · Tohru Konishi · Ayako Yasuda · Masato Matsuura · Nobumasa Kato · Koh-ichiro Yoshiura · Norio Niikawa

Received: 22 November 2006 / Accepted: 13 January 2007 / Published online: 14 February 2007

Abstract Paroxysmal kinesigenic choreoathetosis (PKC) is a paroxysmal movement disorder of unknown cause. Although the PKC-critical region (PKCCR) has been assigned to the pericentromeric region of chromosome 16 by several studies of families from various ethnic backgrounds, the causative gene has not yet been identified. In the present study, we performed linkage and haplotype analysis in four new families with PKC, as well as an intensive polymerase chain reaction (PCR) based mutation analysis in seven families for a total of 1,563 exons from 157 genes mapped around the PKCCR. Consequently, the linkage/haplotype analysis revealed that PKC was assigned to a 24-cM segment between *D16S3131* and *D16S408*, the result confirming the previously defined PKCCR, but being unable to narrow it down. Although the mutation analysis of the 157 genes was unsuccessful at identifying any mutations that were shared by patients from the seven families, two nonsynonymous substitutions, i.e., 6186C>A in exon 3 of *SCNN1G* and 45842A>G in exon 29 of *ITGAL*, which were segregated with the disease in Families C and F, respectively, were not observed in more than 400 normal controls. Thus, one of the two genes, *SCNN1G* and *ITGAL*, could be causative for PKC, but we were not able to find any other mutations that explain the PKC phenotype.

Keywords Paroxysmal kinesigenic choreoathetosis (PKC) · PKC-critical region · Linkage analysis · Mutation analysis · *SCNN1G* · *ITGAL*

T. Kikuchi · M. Nomura · N. Harada · K. Yoshiura (✉) · N. Niikawa
Department of Human Genetics, Nagasaki University Graduate School of Biomedical Sciences, Sakamoto 1-12-4, Nagasaki 852-8523, Japan
e-mail: kyoshi@nagasaki-u.ac.jp

T. Kikuchi
Department of Psychiatry, Nagasaki University Graduate School of Biomedical Sciences, Nagasaki, Japan

H. Tomita
Department of Psychobiology, Graduate School of Medicine, Tohoku University, Sendai, Japan

N. Harada
Kyushu Medical Science, Nagasaki, Japan

K. Kanai
Department of Neurology, Chiba University School of Medicine, Chiba, Japan

T. Konishi
Division of Pediatrics, Nagaoka Ryoikuen, Nagaoka, Japan

A. Yasuda
Department of Pediatrics, Japanese Red Cross Nagoya First Hospital, Nagoya, Japan

M. Matsuura
Section of Biofunctional Informatics, Graduate School of Allied Health Sciences, Tokyo Medical and Dental University, Tokyo, Japan

N. Kato
Department of Psychiatry, Faculty of Medicine, University of Tokyo, Tokyo, Japan

T. Kikuchi · M. Nomura · N. Harada · K. Yoshiura · N. Niikawa
Solution Oriented Research of Science and Technology (SORST), Japan Science and Technology Agency (JST), Kawaguchi, Japan

Introduction

Paroxysmal kinesigenic choreoathetosis (PKC; MIM 128200) is a paroxysmal movement disorder characterized by recurrent and brief attacks of unilateral or bilateral involuntary movements, including dystonic posturing, chorea, athetosis, and ballism, which are precipitated by the sudden onset of movements (Kato et al. 2006). The attacks can last as long as a few seconds to a few minutes, occur up to 100 times daily, but usually manifest in childhood or early adolescents, and commonly decrease with age. There is no loss of consciousness during these attacks. The attacks are responsive to anticonvulsants such as carbamazepine or phenytoin. Electroencephalogram (EEG) analysis demonstrates normal or nonspecific abnormalities. Neuroimaging and neuropathological studies resulted in unremarkable findings (Sadamatsu et al. 1999; Nagamitsu et al. 1999). The etiology and pathophysiology of PKC still remain unclear. Some neurologists consider PKC as a form of reflex epilepsy, whereas others believe that basal ganglia dysfunction may play a role in its cause (Kato et al. 2006). Most (40–70%) were familial cases in which PKC was transmitted in an autosomal dominant mode of inheritance with incomplete penetrance (Tomita et al. 1999; Valente et al. 2000). Males are affected more often than females, with an estimated ratio of 3–4:1 (Bhatia 1999).

We previously performed a genome-wide linkage and haplotype analysis in eight Japanese families with PKC and defined the disease locus within a 12.4-cM region between *D16S3093* and *D16S416* at 16p11.2-q12.1 (Tomita et al. 1999). This PKC-critical region (PKCCR) was confirmed by others (Bennett et al. 2000; Swoboda et al. 2000; Valente et al. 2000; Cuenca-Leon et al. 2002). In addition, mapped regions for other conditions probably allelic to PKC, such as infantile convulsions and paroxysmal choreoathetosis (ICCA; MIM 602066) and benign familial infantile convulsions (BFIC2; MIM 605751), shared with that for PKC (Lee et al. 1998; Hattori et al. 2000; Swoboda et al. 2000; Caraballo et al. 2001; Weber et al. 2004). Nevertheless, mutations in any genes within the PKCCR have remained uncovered.

Here, we describe the results of the mutation analyses of seven PKC families for a total of 157 genes located at or around the PKCCR, together with linkage/haplotype analysis of four newly identified families.

Materials and methods

Subjects

The subjects studied included seven families (Families A–G) with PKC. Two of them (Families F and G) corresponded respectively to Families 1 and 3 in our previous report (Tomita et al. 1999), and five other families (Families A–E, Fig. 1) were those which were newly collected. A total of 21 members, including 16 PKC patients from four of the five families (Families A–D), underwent a linkage and haplotype analysis. In addition, one of each affected individual (we further call them representative patients) chosen from all seven families was subjected to mutation analysis. Blood samples were collected from all participants after obtaining written informed consent, and the study protocol was approved by the Committee for Ethical Issues on Human Genome and Gene Analysis at Nagasaki University.

Genotyping and linkage analysis

Genomic DNA was isolated from the blood lysate of the 21 participants by phenol-chloroform extraction, followed by ethanol precipitation. To try to narrow down the PKCCR, we performed genotyping and haplotype analysis in the four newly collected PKC families, using 13 microsatellite markers (Table 1) located to a 36-cM region at 16p12-q21 to which PKC has been shown to be linked, as well as using three

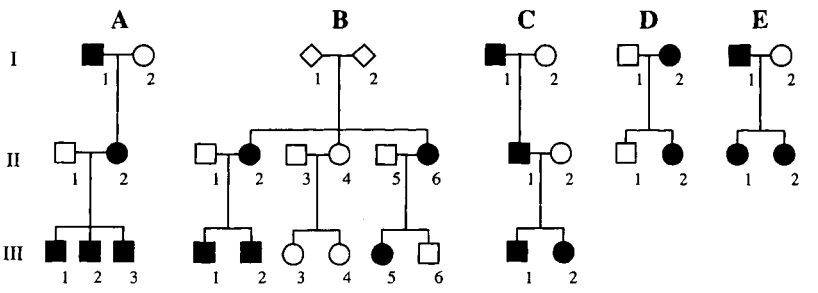

Fig. 1 Pedigree of the five families (Families A–E) with paroxysmal kinesigenic choreoathetosis (PKC). The *closed squares* and *circles* denote individuals affected with PKC. Although not shown here, Families F and G correspond to Families 1 and 3 reported previously (Tomita et al. 1999)

Table 1 Primer sequences of the 12 microsatellite markers used for genotyping and linkage analysis

Markers	Forward primer (5′–3′)	Reverse primer (5′–3′)
D16S403	CAAGACTAACGCTGATGGCT	GACAGTGAGGTGGGAATCAAA
D16S417	CTGTCCAACATGCAGCC	TGAAGTCAATCCCACTTGAA
D16S3131	CTGCTTCCATCTTGCC	CTAGCCCCCAAATGTG
D16S3093	CAAGGGCAAAACTCCAT	CCAAAAGGTTGATTCTCTG
AC007353-M1	GCTTAACTACATTTTATTCAAGGTTG	TCTGTGGTAGAGAGGCAAAGA
AC092368-M1	GTTTACCAGCCATTTTTAATCAACA	TGAATAAGTGTGTCTTTCAACAAAATT
AC092721-M3	GCCCTGTAATATAATTTGAAGTTG	GGGTTCAAGTGATTCTCCTG
D16S3136	CTCACCTATTGCCCTCAAGAA	CAGAATCTTATGCCATTATT
D16S416	CATAGGACCCTCAGATGTATA	CTGCCTATGGCTAAGAGGACA
D16S408	TGTAACCTTGTGTGCATCCT	CACTCTTATCCCAGGAACCC
D16S514	CAATTCCTTGATGCTACCAT	CTTGTCTAGTGGCTGGAATA
D16S3143	GCTACTGAGGAAACCTTATCC	GGCCATTACAGGAAGTGC

Primers of D16S3068 were purchased from the ABI PRISM Linkage Mapping Sets LMS (Applied Biosystems, Foster City, CA)

additional markers (AC007353-M1, AC092368-M1, and AC092721-M3) that were designed by us according to the human genome sequence (http://genome.cse.ucsc.edu/). Sample DNA was polymerase chain reaction (PCR) amplified for each marker locus with fluorescence-labeled primers. PCR was performed on DNA Thermal Cycler Model 9700 (Applied Biosystems, Foster City, CA) in a 10-μl reaction mixture containing 1×PCR buffer (Takara Bio, Otsu, Japan), 200 μM each of dNTP, 0.5 μM each of primer, 10 ng DNA, and 0.25 units ExTaq DNA polymerase HS-version (Takara Bio, Otsu, Japan) under the conditions of denaturation at 94°C for 2 min, 35 cycles of 94°C for 30 s, 58°C for 30 s, and 72°C for 1 min, and final extension at 72°C for 7 min. PCR products were run on an auto-sequencer Model 3100 (Applied Biosystems, Foster City, CA). Allele sizes were analyzed by GeneScan and Genotyper software (Applied Biosystems, Foster City, CA) to determine the genotypes.

Mutation analysis

We performed PCR-based mutation analysis of the seven representative patients with typical features of PKC. Sequences examined for mutations among the seven patients included those of 1,371 coding exons, excluding the 3′-UTR and 5′-UTR in 117 genes, located at the PKCCR between *D16S3093* and *D16S416* (Table 1). The analysis in five families (Families A and C–F) was expanded to an additional 192 exons of 40 other genes, whereas because of depletion of genomic DNA, an expanded analysis was not done in the remaining two families. Thus, a total of 1,563 exons in 157 genes were analyzed for mutation (primer sequences are available on request).

Real-time quantitative PCR

We performed real-time quantitative PCR in six representative patients from Families A and C–G. Six pairs of primers and TaqMan probes were designed for exons 1, 6, and 13 of *SCNN1G*, and for exons 1, 16, and 30 of *ITGAL*. PCR was carried out in a 10-μl reaction mixture containing 5 μl of 2×TaqMan Universal PCR Master mix (Applied Biosystems, Foster City, CA), 0.4 μM each of primer, a 0.2-μM probe, and 10 ng DNA under the conditions of 2 min at 50°C, 10 min at 95°C, 40 cycles of 15 s at 95°C, and 1 min at 60°C, with a 7900HT Sequence Detection System (Applied Biosystems, Foster City, CA).

Results

The haplotype analysis showed that all affected individuals in the four new families share an allele at each locus examined between *D16S3131* and *D16S408* (Fig. 2). One end of the shared region was defined by a recombination between *D16S3131* and *D16S3093* in individual III-3 in Family A, and the other end by a recombination between *D16S514* and *D16S408* in individual III-1 in the same family. These results defined a minimum PKCCR in the four new families within an approximately 24-cM segment between *D16S3131* and *D16S408*. Therefore, the present linkage/haplotype analysis did not contribute to narrow down the previously defined PKCCR.

Among a total of 1,563 exons of 157 genes analyzed, we detected 243 base alterations in the seven representative patients (Fig. 3), 36 of which were base substitutions in coding regions and have not been reported in the dbSNP database (http://www.ncbi.nlm.-

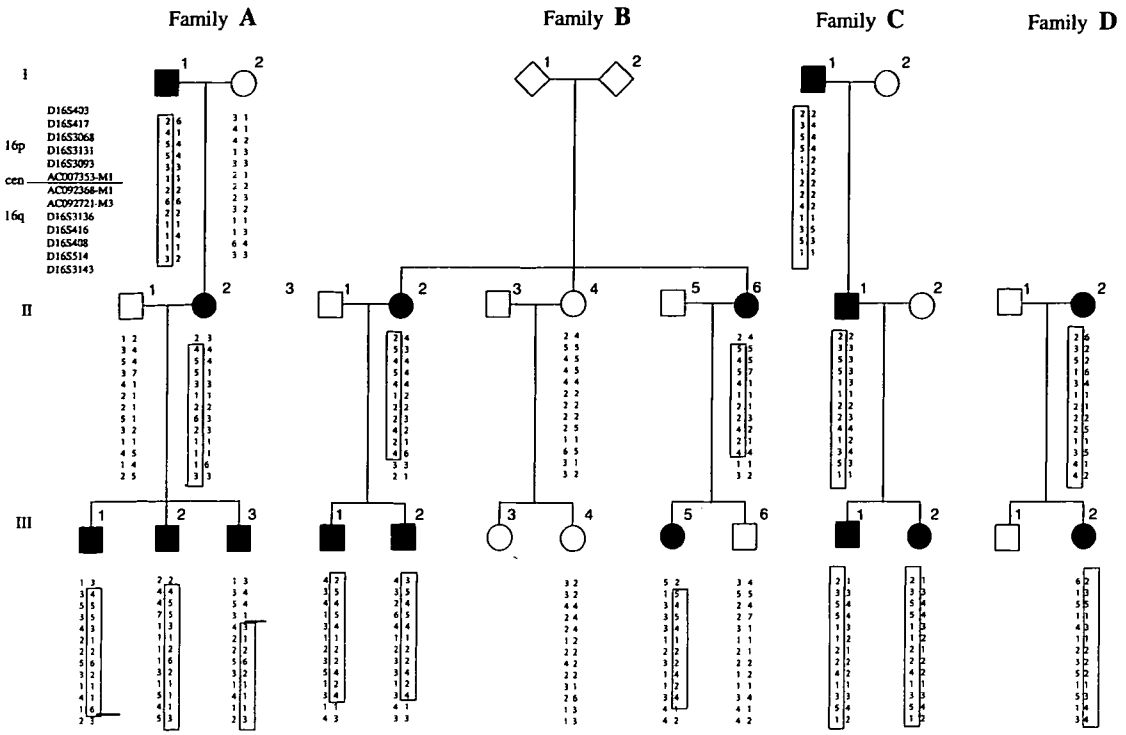

Fig. 2 Haplotype analysis of the four new PKC families (Families A–D). The *numbers in boxes* represent putative disease haplotypes. The *heavy short lines* indicate recombination sites

nih.gov/SNP/). Seven of the alterations in six genes were nonsynonymous substitutions resulting in amino-acid substitutions (Table 2). Five of such nonsynonymous substitutions in four genes were observed both in some patients and among 100 normal control individuals. The remaining two, i.e., 6186C>A in exon 3 of *SCNN1G* (the gene for sodium channel, nonvoltage-gated 1, gamma) and 45842A>G in exon 29 of *ITGAL* (the integrin alpha L precursor gene), observed in Families C and F, respectively, were not observed among more than 400 normal controls. The real-time quantitative PCR analysis did not detect a duplication or a deletion within the two genes. Of the 35 intronic base changes we identified in the seven patients, none were located at the acceptor or donor splice sites (Fig. 3).

G-banding chromosome analysis at the 400-band level and C-banding analysis revealed that all five patients from Families B–D, F, and G had a normal-sized heterochromatin block on chromosome 16 without an inversion (data not shown).

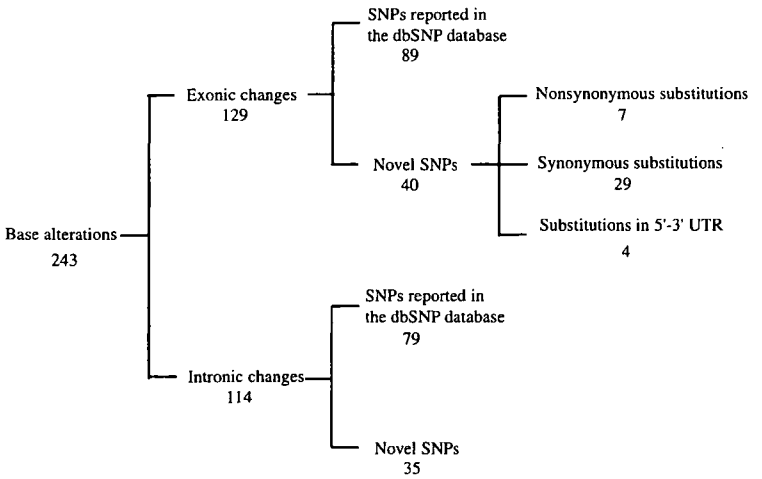

Fig. 3 Classification of 243 base alterations in 157 candidate genes. Information of the newly found single nucleotide polymorphisms (SNPs) is shown in Table 2. None of the novel intronic SNPs are located at any of the acceptor or donor splice sites

Table 2 List of genes for mutation analysis in the PKC patients, and novel SNPs identified, their positions, nucleotide changes, and amino acid changes

Gene	E/I	SNP definition	AA	Gene	E/I	SNP definition	AA	Gene	E/I	SNP definition	AA
HS3ST2*				ASPHD1	E1	515insTGG		ITGAX*			
SCNN1G*	E3	6185G>T	Y241Y	KCTD13*	I2	INV2-74A>T		ITGAD*	5′U	5′U-13G>C[a]	
	E3	6186C>A	P242T	LOC124446					E2	943C>T	G33G
SCNN1B*				TAOK2*					I7	INV7+38C>T	
UBPH*				HIRIP3*					E8	14188A>G	R246R
NDUFAB1*				CCDC95					E8	14253A>G	Y268C
PRKCB1*	E1	79C>A	R27R	DOC2A*					I9	INV10-43G>A	
	I15	INV15+85G>T		FAM57B	I2	INV2+66G>T			E16	19819A>G	S644G
CACNG3*				ALDOA*					I17	INV17+139G>A	
TNRC6A*	E1	5′U-12079T>A		PPP4C*	E1	5′U-355-347del(CGG)3			I19	INV19+71C>T	
	E21	33511C>T	H1551H	TBX6*					I27	INV27+87G>A	
SLC5A11*	I1	5′U-12193T>C		YPEL3*				ARMC5*			
	I2	INV2+6C>G		GDPD3				TGFB1I1*	E5	753C>T	P119S
	I5	INV5-30G>A		MAPK3*				SLC5A2*			
	I5	INV5+65T>C		CORO1A*				C16orf58*	I5	INV5+53G>A	
LCMT1*				SULT1A3*				ERAF*	3′U	3′U+570T>C[a]	
IL4R*	I3	INV3+72T>A		CD2BBP2*	I1	INV1+493C>T		MGC3020*			
	E11	22448T>C	L433L	TBC1D10B*				ZNF720*			
IL21R*	I4	INV4+51C>T		MYLPF	I5	INV5+27G>A		ZNF267			
GTF3C1*				SEPT1*				TP53TG3*	E3	1232insG	
KIAA0556*	I16	INV16+4T>C		ZNF553	E2	2434G>A	T326T	FLJ43855			
	E18	204044A>G	Q1198Q	ZNF771				POL3S			
GSGIL*				XTP3TPA*				FLJ46121			
XPO6*	I9	INV9+31insT		SEPHS2*				FLJ43980	E1	5′U-15C>G	
	I15	INV15+23G>C		ITGAL*	E1	5′U-86C>T		SHCBP1*	E5	12986C>T	N204N
	E16	69120T>C	N740N		E29	45842A>G	K1063R	VPS35*			
SBK-1				ZNE768				ORC6L	E6	6328A>G	V193V
LOC440350				ZNF747				MLCK*			
LOC440348				ZNF764				LOC388272*			
CLN3*	I12	INV12+36C>T		ZNF688				GPT2*			
	E15	14138A>G	H404R	ZNF785				DNAJA2*			
APOB48R*				ZNF689				NETO2*	I3	INV3-34G>A	
IL27*	I5	INV5-12C>T		PRR14				ITFG1 *			
NUPR1*				FBS1*				PHKB*	I28	INV28+37C>T	
CCDC101*				SRCAP*				ABCC12*			
SULTIA2*				PHKG2*				ABCC11*			
SULT1A1*				LOC90835				LONPL*			
EIF3S8*	E16	20499C>T	P725P	RNF40*				SIAH1			
ATXN2L*	I13	INV13+55G>A		BCL7C*				N4BP1*			
TUFM*				CTF1*				CBLN1*			
SH2B*				LOC283932				FLJ44674	E1	3′U+905C>G	
ATP2A1*				FBXL19*				C16orf78*	E1	45G>A	K15K
RABEP2*	I3	INV4-56C>T		TMEM142C					I3	INV3+27A>G	
CD19*	E4	1379G>T	P206P	SETD1A*				ZNF423 *			
SPIN1*	E7	6897C>T	S319S	HSD3B7*				C16orf69			
	I7	INV7+278Cdel		STX1B2*				HEATR3 *	I11	INV11-44A>G	
	3′U	3′U+9285C>A[a]		STX4A*	I8	INV8+55C>A		PAPD5*			
LAT	E7	1259G>A	A120A		I8	INV8+65C>T		ADCY7*	E22	24951T>C	Y875Y
BOLA2				ZNF668				BRD7*	I9	INV9-26insT	
GDYD1*				ZNF646*	I1	5′U-108T>G			E16	48481G>A	T570T
SPN*					E2	2722G>C	G907A	NKD1*			
QPRT*				VKORC1*	3′U	3′U+3730G>C[a]		SLIC1*			
C16orf54				BCKDK*				CARD15*			
KIF22*	I12	INV12+70A>G		MYST1*				CYLD*	E17	43909C>T	D805D
MAZ*				PRSS8*	E3	2163C>T	V46V	SALL1*			
PRRT2				PRSS36				FTS*			
MVP*	E10	11504C>T	D525D	FUS*				CAPNS2*			
C16orf53				TRIM72				SLC6A2*			
CDIPT*				PYCARD*				GNAO1*			
PSK-1*				PYDC1*				CNGB1*	E22	51134C>T	N725N
				ITGAM*	I2	INV2+11T>C					

A total of 75 SNPs not reported in the dbSNP database were found in this study

Four SNPs found in 5′-UTR or 3′-UTR happened to be included in the sequenced regions

*Analyzed in seven representative patients: E/I=exon or intron; AA=inferred amino acid change from nonsynonymous SNP; U=UTR

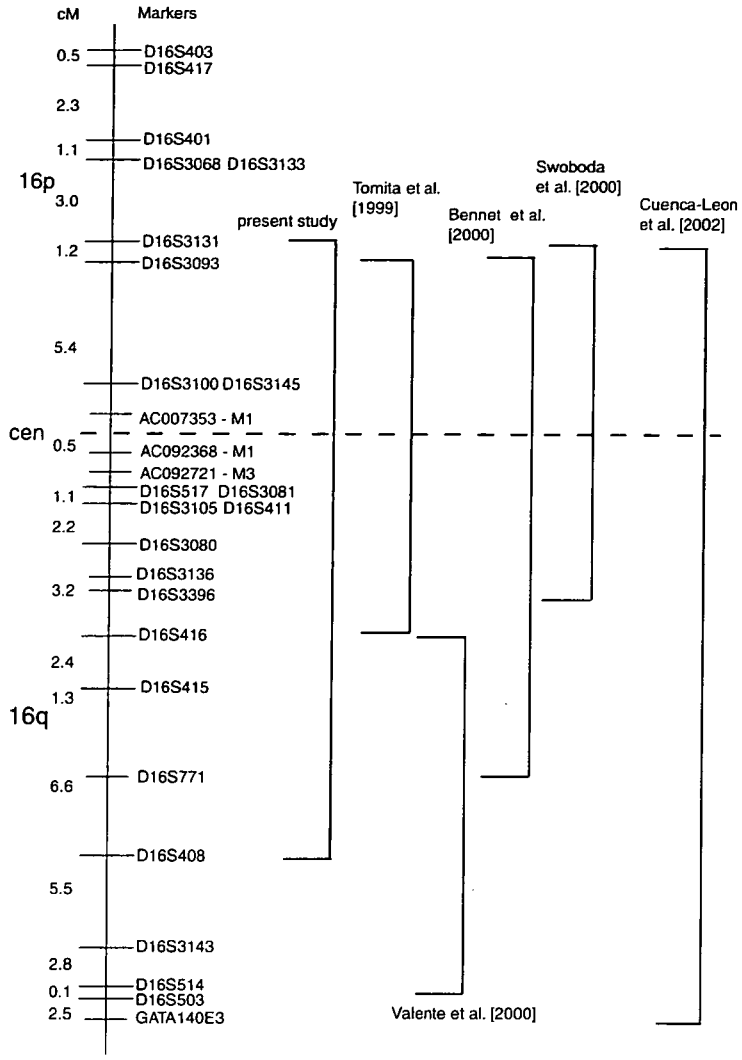

Fig. 4 The PKC-critical region (PKCCR) summarized by five mapping studies (Tomita et al. 1999; Bennett et al. 2000; Swoboda et al. 2000; Cuenca-Leon et al. 2002, present study), as well as a seemingly second PKC locus (EKD2) by Valente et al. (2000). The location of markers and intermarker distances are from the Généthon map (Dib et al. 1996)

Table 3 List of exons that have not been sequenced in the mutation analysis

Gene	Exon
COX6A2	Exon 2, Exon 3
MAZ	Exon 1, Exon 2, Exon 3
VPS35	Exon 9, Exon 10, Exon 11
SULT1A1	Exon 7
SALL1	Exon 2
MGC2474	Exon 2
FLJ43855	Exon 5, Exon 7, Exon 9

Discussion

The PKCCR was assigned to a segment between *D16S3093* and *D16S416* in eight Japanese families (Tomita et al. 1999). It was also mapped between *D16S3100* and *D16S771* in an Afro-Caribbean family (Bennett et al. 2000), between *D16S3131* and *D16S3396* in 11 families of diverse ethnicity (Swoboda et al. 2000), between *D16S3145* and *GATA140E03* in a Spanish family (Cuenca-Leon et al. 2002), and a 24-cM segment between *D16S3131* and *D16S408* in the present study (Fig. 4). Thus, the shortest region of overlap (SRO) did not become narrower than a 12.4-cM segment detected by Tomita et al. (1999). Valente et al. (2000) assigned a form of PKC (a second PKC locus, EKD2), in an Indian family, to a segment between *D16S416* and *D16S503*, the region distinct from those mapped by Tomita et al. (1999) and by Swoboda et al. (2000). Furthermore, two other clinical entities, ICCA and BFIC2, were assigned to a region encompassing the centromere of chromosome 16 (Lee et al. 1998; Hattori et al. 2000; Swoboda et al. 2000; Caraballo et al. 2001; Weber et al. 2004). Since all of these loci were confined to a relatively small region, it is likely that all of these paroxysmal movement dis-